Modular Timber Structures with Parametric Design Frameworks

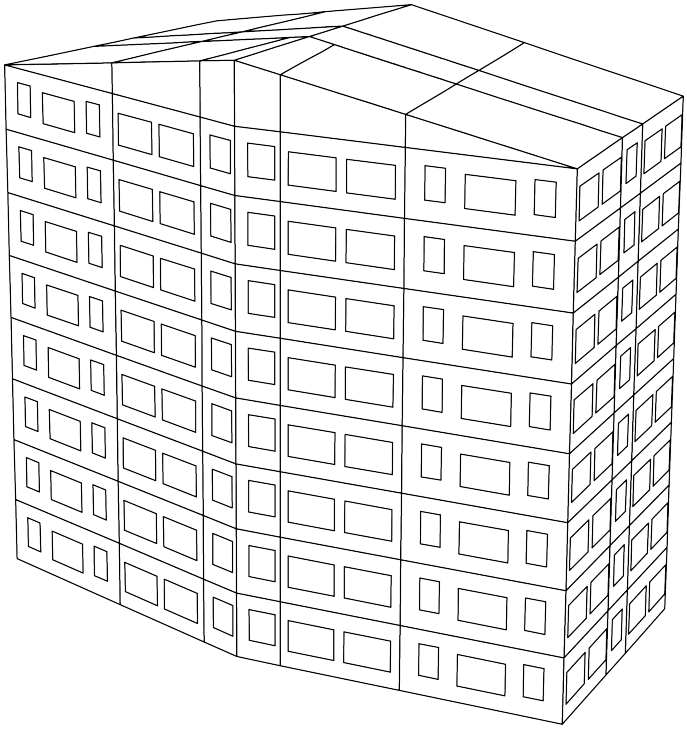

Master Thesis Project

Simon Clavelin

June 2017

Technical University of Denmark
Department of Civil Engineering
Brovej, Building 118
2800 Kgs. Lyngby
Denmark

Author:

Simon Clavelin
s151369

Supervision:

Kristoffer Negendahl
Department of Civil Engineering

Preface

This Master Thesis is submitted as partial fulfilment of the requirements to the obtention of the degree of Master of Science in Architectural Engineering, from the Technical University of Denmark. The work that it presents has been developed within the Department of Civil Engineering, in collaboration with the STED Network. It accounts for 30 ECTS credits on a total of 120, and was carried out over a period of 5 months, from January 23rd, 2017 to June 23rd, 2017.

I would like to express my gratitude to Kristoffer Negendahl, my supervisor, for his guidance during this project. His invaluable ideas, suggestions and enthusiasm helped me ask myself the right questions and strive towards the exploration of new horizons.

I would also like to thank my parents and family for their continuous support and caring during this journey.

Last but not least, I address my thanks to my friends for their daily companionship, advice and listening, who contributed to make these 5 months thoroughly enjoyable.

Kongens Lyngby, June 23rd, 2017

Simon Clavelin

Abstract

Massive timber is shaking current construction standards by introducing new concepts that are not only more sustainable, but also have the potential to outperform traditional techniques. This master thesis focuses on a component of this family, Cross Laminated Timber (CLT), which thanks to a high dimensional stability in-plane, is pushing the limits of what can be achieved with timber buildings.
The work presented in this report has the ambition to contribute to the democratisation of CLT, by making its structural design accessible to a broader audience. To this end, a novel approach to the structural verification of CLT buildings is proposed through an integrated dynamic model, which links a geometry tool and a structural analysis tool in a single model by means of parametric design. The framework is inspired by prefabrication and modular techniques employed by the CLT industry, and defines a methodology to lead designers from the geometry creation to the structural analysis results, oriented towards the early phases of building design. It has been devised to deliver a wide range of visual and textual feedback, as well as decision help support.
The structural design of CLT is based on the material properties and analyses developed by TU Graz, and proposes the assessment of horizontal deflections, CLT walls loaded in-plane and CLT floors loaded out-of-plane. An equivalent isotropic modelling of CLT panels is investigated; its validity is evaluated in comparison with an orthotropic modelling via FEM simulations. It has been found that such modelling has a considerable influence on the analysis results, and that orthotropic materials will likely be subjected to higher displacements and concentrated stresses. In an attempt to compensate for this, safety factors are suggested.
In the end, it is thought that such framework can bring a better understanding of CLT structures in a user-friendly, flexible environment which supports the multiple design iterations characteristic from the early design stages.

Contents

List of Figures

List of Tables

Chapter 1

Introduction

With environmental concern gaining momentum in society, architects and engineers try to find ways to reduce the environmental footprint of new buildings. This sparkles an interest in sustainable materials, bringing forward a renewal of the timber age. At the heart of this revolution lie Engineered Wood Products such as Glued Laminated Timber and Cross-Laminated Timber, defining a new technique called massive timber construction. This technique allies the natural qualities of timber with engineering, and make possible the realisation of pioneering projects that push further the limits of building design.

1.1 Massive timber and the Nordic countries

The Nordic countries, especially Norway, Sweden and Finland, hold a strong tradition of using wood in building construction. Thanks to a readily available natural resource and an abundance of forests, timber is dominating the market in single family houses at about 90%, even though multi-residential housing does not follow this tendency, with approximately 7% share in Sweden, for example [1].

However, thanks to increasingly more demanding environmental regulations, massive timber use is growing and starts gaining in popularity, especially with products like CLT which showcase competitiveness regarding materials such as concrete. Notably, this led to the Nordic Wood programme which aimed at developing experimental massive timber projects between the five Nordic countries.

Regarding CLT in particular, producers start to be established in Scandinavia, for example with Martinsons[1] (Sweden) and Oy Crosslam Kuhmo (Finland) [2]. The production remains relatively small, however, in comparison to the biggest producer in Europe, Stora Enso, based in Austria; a considerable amount of CLT in still being imported from leading countries to undertake timber construction projects.

Among current developments, some Nordic projects stand out remarkably among the most innovative in the world, as evidenced by the *Treet* by the Bergen and Omega Building Society (BOB), a 14-storey timber building in Bergen (Norway) said to be the tallest timber building in the world (49 meters high) [2].

[1] https://www.martinsons.se
[2] http://www.crosslam.fi/en/

Figure 1.1.1: The *Treet* building in Bergen, Norway (Image: CTBUH Global News)

The apartment block consists in a hybrid structural system of massive timber, using Glulam elements and stacked prefabricated modules. The timber structure is so light that concrete had to be added on top of the 5^{th} and 10^{th} to increase the weight and reduce the influence from the wind. While such project was initially more costly than traditional concrete/steel structure, the prefabrication allows for a very short erection time, at a pace of 4 stories in only 3 days [2].

Another project in Trondheim (Norway), *Moholt 50/50* by MDH Arkitekter, made headlines as the worlds largest CLT complex in Europe [3]; similarly, White Arkitekter has been selected to design the Kulturhus in Skellefteå (Sweden), a hybrid timber-framed high rise featuring supporting steel and a concrete core [4].

Figure 1.1.2: Moholt 50/50 by DMH (Trondheim, Norway) [5] and the Kulturhus in Skellefteå (Sweden) [4] by White Arkitekter

Despite this, in Denmark, the evolution of massive timber projects is slowed down in favour of a long time history in precast concrete construction. Due to less available timber resource and a wish

to decrease risks and maximise profit, the latter has become a dominant technology and makes up for 90 to 95 % of the new build.

Yet, the city of Copenhagen announced its plan to become the world's first carbon neutral city by 2025, as well as having developed an additional 6.8 million m^2 of new buildings. According to a study by Horswill and Nielsen (Søren Jensen consulting engineers) [6], switching from precast concrete to massive timber (especially CLT) for only 1 out of 6 new residential building would greatly serve this ambition, with a contribution of up to 22% each year to reduce Copenhagen's CO_2 deficit (70 000 tons). This calculation takes into account the assessment of cradle-to-gate concerns, transportation and end-of-life, as well as the reduction of concrete to be used for the foundations.

Still, this cannot be achieved without a real strive towards sustainability and the evolution of governmental regulations, and the barriers towards adoption of this new system are many. For massive timber projects to flourish, the construction industry and clients have to be willing to embrace this new building technique, which does not come without difficulty. Contrarily to well established skills and processes regarding precast concrete (PC) solutions, CLT is confronted to a perceived increased risk and costs [6], making it unlikely to be chosen over PC without the existence of regulation, incentives or a client direction.

Perceived as the major barrier, the limitations imposed by building regulations make the implementation of tall timber buildings difficult, especially regarding fire and seismic safety [7]. For example, current danish fire safety regulations prohibit the construction of timber building of more than 4 stories [6]. In comparison, this ban has been lifted in 1994 in Sweden [8] and in 1997 in Norway [9].

A demand for maximum profit and resource efficiency is also likely to make the shift towards massive timber construction more difficult. Horswill and Nielsen [6], while discussing the development of a post PC industry in Copenhagen, found out that CLT could lead to a cost rise of 26% compared to current building techniques employed by the Danish industry. Among the contributing factors to this increase is the fact that no CLT industry is existing yet in Denmark, meaning that CLT products would have to be shipped from Austria, whereas concrete is mostly produced locally.

Regulations and economic considerations let aside, there is one more crucial argument that might explain why massive timber construction is still beyond reach in Denmark. According to a survey by Espinoza et al. [10], the level of awareness of CLT among contractors and construction managers is "low" to "very low" for around 95% of the respondents. Architects and engineers are also concerned, with only 28% and 32% possessing high to very high awareness of this product. The latter are indeed more comfortable with other materials such as steel and concrete [7], which are well framed within the European normative and more commonly taught during their respective educations [1]. In comparison, CLT was subjected only recently, in 2014, to the first European Standard EN 16351 [11]; its apparition in the next revision of the Eurocode 5 [12] remains to be seen. Therefore, when large scale timber structures are attempted, this can lead to catastrophic failures, such as the one of the Siemens Arena (Ballerup, Denmark, in 2003). Even though the cause is nearly always due to limited competence about timber constructions [1], such events are unlikely to appease the global perception of a riskier system to work with.

1.2 Motivation and problem definition

Technology transfer and knowledge gaps have thus a considerable impact on the democratisation of massive timber construction. Despite a strong will to aim for a sustainable future, such initiative is subjected to a lack of awareness towards relatively new materials, which furthermore challenge an established industry.

If we wish to see more groundbreaking timber projects within the next years, it is necessary to dismantle common misconceptions about these techniques, but also empower professionals over their use. Provided with a better understanding of their principles, as well as relevant tools to guide them, designers can be a major driving force behind the transition to massive timber.

This calls for an integrated process between multiple disciplines, architects as engineers, from the early design stages where the choice of a structural system is evaluated.

This thesis has the ambition to contribute to this movement, by developing an alternative framework for the structural design of massive timber buildings, with an exclusive focus on Cross Laminated Timber (CLT).

The framework differentiates itself from common procedures by a wish to make structural design of CLT accessible side by side with architectural design. Aided by parametric design, its goal is to integrate geometry creation, typically performed by architects, and structural performance feedback in a single, flexible environment with a quasi-instantaneous exchange of information.

The ultimate goal of this work is to promote the emergence of *hybrid practitioners* who possess "equal insight in technical analysis as well as architectural design" [13], armed with confidence when it comes to initiate architectural projects with Cross Laminated Timber.

Emerging from this motivation, the interrogations that this report will attempt to solve are the following:

- Is it possible to design a method providing the flexibility required by early design stages?
- Can it deliver relevant feedback to help designers grasp the principles of CLT?
- Can parametric design reflect the complexity of CLT materials?

To answer these questions, the principles and structural design of CLT will be investigated firsthand, to serve as a basis for the framework. The latter will then be crafted and its validity evaluated with a FEM software. Finally, the method is applied on an existing case study, the Puukuokka housing block by OOPEAA.

1.3 Collaborative Framework - Nordic Built and STED

This thesis has been carried out in collaboration with the STED Network, part of the Nordic Built programme.

The Nordic Built programme took shape under the impulsion of Nordic Ministers for Trade and Industry, and gathers all five Nordic countries under a common goal of sustainable solutions for the built environment.

It is comprised of three modules: the *Charter*, which provides a collaborative platform and defines ambitions for the programme; the *Challenge*, oriented towards the development of sustainable refurbishment concepts; and the *Change*, researching new concepts oriented towards sustainability.

The STED Network, which stands for Sustainable Transformation and Environmental Design [14], is part of this last module. The project was launched by the Technical University of Denmark in 2015, and involves several universities and architecture studios from the Nordic countries. Its focus is the development of new tools oriented towards Life Cycle Analysis (LCA) and sustainability evaluation within the early design phases.

One of the collaborators of the STED Network is OOPEAA, or Office for Peripheral Architecture, an architectural studio based in Finland. OOPEAA provided drawings from their housing project *Puukuokka*, which will serve as a case study for the implementation of the framework.

1.4 Structure of the Thesis

This thesis is divided in three separate entities, which can be read individually yet reference and complement each other.

The first one, namely this present report, consists in 6 main chapters, numbered from chapter 2 to 7. First hand, Chapter 2 brings a general overview of the CLT materials, specifying their characteristics and properties. Chapter 3 goes deeper into the structural verifications that must be considered with CLT. In Chapter 4, the framework is developed; its objectives, limitations and assumptions are underlined, and this approach is evaluated in Chapter 5. Chapter 6 showcases the structural feedback which is delivered to the user. Finally, the relevance of the framework is discussed in Chapter 7.

The second book, "Framework Manual", consists in an illustrated guide to the framework, to the attention of users. It explains the different components that were developed, further details the assumptions of the final model and aims at providing knowledge on how to operate it, to obtain the desired results.

Finally, the third and last book "Appendices" compiles additional data including simulation results, the framework's spreadsheets and its parametric components.

Chapter 2

Cross Laminated Timber Technology

This chapter introduces the main characteristics of CLT, its current development and assets. The behaviour of CLT structural systems is briefly discussed in comparison with other timber and concrete techniques.

2.1 Cross Laminated Timber: An overview

Cross Laminated Timber (CLT) is a engineered massive wood product, made up of an uneven assembly of timber layers, arranged crosswise to each other at an angle of 90°. The layers are then connected in a quasi-rigid manner with adhesive bonding to produce a material suited for bearing loads in and out of plane [15].

Figure 2.1.1: CLT panels [16] and illustration of the layers arrangements [17]

2.1.1 Brief history

It was first developed in Austria and Germany as a way to find a better use for side boards, which were regarded as having little value. Nevertheless, their mechanical properties are known to be higher, which has turned out to be beneficial to produce the solid material first defined as "Brettsperholz" by Dröge and Stoy in 1981; the current English term CLT has been introduced in 2000 by Schickhofer and Hasewend (cited in [18]).

Following developments initiated by the Graz University of Technology in the 1990s, first technical approvals were issued around 1998. From then on, its volume production kept on growing to reach nearly 700 000 m^3 worldwide at the end of 2015 [18]. The characteristics of the product are now governed by the European Standard EN 13651 [11], voted in 2014, and its inclusion in the next revision of the Eurocode 5 is underway.

2.1.2 CLT layup configurations

In its minimal form, CLT accounts for at least three layers with a thickness varying between 6 and 45 mm [11]; this number usually grows up to 7 layers, or even 11 in some cases. Due to its composite nature, a wide range of layup arrangements is imaginable. In general, graded solid timber layers (principally softwood species such as Norway spruce [15]) constitute most of its thickness, although engineered products such as laminated veneer lumber (LVL) or oriented strand boards (OSB) can be used for up to half of the total thickness. For CLT elements with at least 4 layers, it is even possible to propose variations with adjacent layers glued parallel to the grain, within the limits imposed by the normative EN 13651 [11].

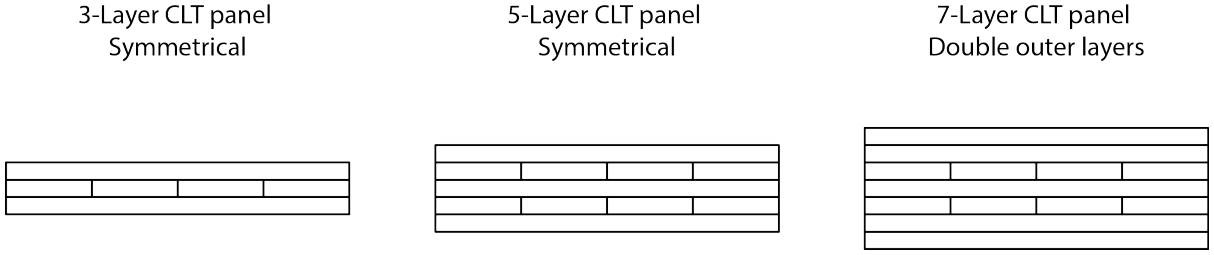

Figure 2.1.2: Different CLT layup configurations

2.1.3 Manufacturing process and dimensions

Cross Laminated Timber relies on the assembly of several timber lamellas. In order to homogenise the product and remove defects that can occur in the log (e.g. knots), the latter are finger jointed to obtained the desired panel dimension. They can then be arranged in crosswise layers and surface bonded with adhesive such as melamine urea formaldehyde (MUF), and pressed together either by hydraulic or vacuum equipment [15].

Nonetheless, this implies that there might be gaps between boards in the final product of up to 6 mm [11]. To improve the properties of CLT regarding building physics (e.g. air tightness, acoustic insulation or fire design [18]), manufacturers aim to reduce these gaps as much as possible by going through the additional step of edge bonding the boards together. Single layers of solid glued timber are therefore produced before being face bonded crosswise.

In case where openings are needed for e.g. windows or staircases, these are cut through the panel, making it a subtractive process; manufacturers usually charge the gross area of the panel. Additional fitting of panels can include bending to produce curved geometries.

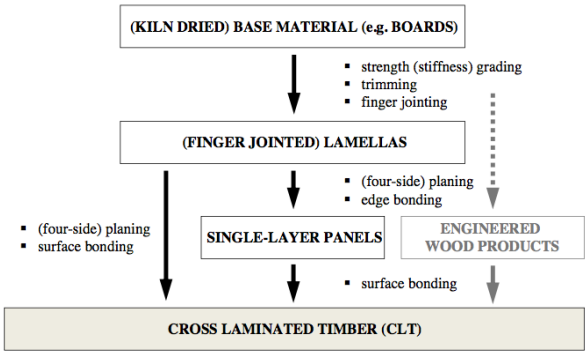

Figure 2.1.3: Overview of CLT's manufacturing process [15]

CLT can be manufactured in large dimensions to support the production of wall and floor elements, though linear components such as beams can also be realised [15]. Panels are nowadays commonly manufactured within lengths up to 18m, widths up to 4m, and thickness up to 0.4m, though the recent normative [11] allows thicknesses up to 0.5m. As far as the two first dimensions are concerned, they are limited mostly by the manufacturer, but also by local regulations such as a country's size limits for road transportation and the transportable weight [19].

2.2 Advantages of CLT products

First and foremost, as environmental concerns grow, it is desirable to turn to materials with a reduced carbon footprint. Sustainability has been cited as the strongest motivation for adoption of CLT products [7]. Comparatively to structural materials fulfilling a similar function, such as concrete, CLT is said to have a potentially beneficial footprint. Indeed, wood acts as a carbon sink: it absorbs CO_2 within its life cycle. CLT contains more carbon in the product than what is emitted during its manufacturing. This helps the climate change mitigation, even though this carbon storage will eventually be released in the future [17].

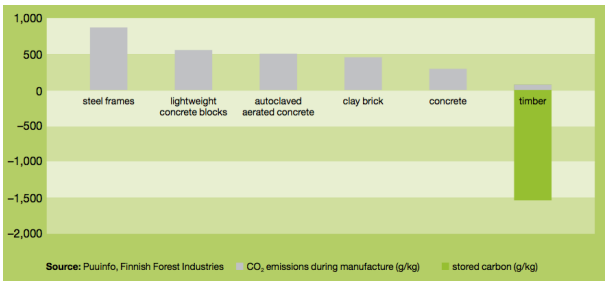

Figure 2.2.1: Carbon emission of CLT vs. other building materials [20]

After being disassembled, the timber material can also be used as a replacement to fossil fuels to produce energy. Other aspects that can be noted is a favourable impact on indoor environment and the users' health in general [21].

This is not the sole benefit of CLT, which is a very versatile material. Assembled in factories, the product in itself is perfectly suited for prefabrication, reducing drastically the erection times on site by bringing large pieces together. It makes for a clear separation between layers of construction

(structure, insulation, piping, etc.), making the construction easier, and has a low air permeability.

On the structural point of view, the arrangement of crosswise layers provides CLT with a very good dimensional stability in plane, reducing swelling and shrinkage in comparison to other wood products. In addition, CLT panels behave very well under in and out-of-plane loads, making it suitable for use as floors and walls. It also provides a light weight structure that will fit building sites with a soil showing weak bearing capacity: it is indeed, in terms of weight, six times more efficient than concrete panels [22]. While current regulations in Denmark hinder its development on fire safety grounds, CLT (and timber in general) behave well in a fire, thanks to a self-protecting charring. It can therefore be left uncovered provided that the structural design takes this factor into account.

Finally, its important stiffness can be exploited as a stabilising structure against horizontal loads, without the need to add a sheathing layer as it is the case with timber frame constructions. This achieves to make it a "high-value alternative" to mineral-based solid construction materials [18] when it comes to mid-rise buildings.

CLT's popularity also grew among architects and designers. Contrarily to standard timber frame construction, the windows can be placed freely and are not restricted to a grid, thanks to the crosswise arrangement of layers. It can also provide a warm interior finish when left uncovered, and is known to have positive impact on the quality of life of the inhabitants.

2.3 Building systems in CLT

As introduced above, CLT projects rely heavily on prefabrication. The manufacturing process benefits from a 'file-to-factory' integration [8], taking it directly from the design drawings to the delivery of panels with very reliable precision. While the initial product cost is higher, this asset helps bringing it down to competitive levels compared to non-prefabricated building techniques, due to highly reduced erection times. To further emphasise this aspect, companies such as Stora Enso developed entirely customised building systems in CLT, delivered as finished products on site. Such systems are especially suited to multiple repetition of identical elements.

Traditional prefabrication, also called 2D prefabrication, consists in assembling single elements in the factory. Walls and floors built this way are shipped and assembled on site. This allow designers to exploit the entire range of products provided by the manufacturer, without major limitations.

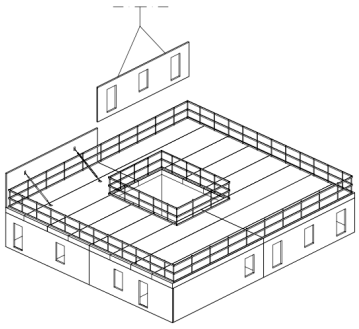

Figure 2.3.1: Assemblage of a prefabricated CLT wall

This technique is very much like other already existing prefabricated methods (e.g. prefabricated concrete).

What brings CLT and timber systems in general beyond this technique is the fact that timber is extremely light compared to reinforced concrete, with a density of ≈ 4.2 kN/m^3 against 25 kN/m^3. Timber structures have thus the possibility to upgrade to a modular level of prefabrication. Modular elements are composed of structural elements (floors and walls), but are also fitted with building services equipment, internal and external finishes, and so on.

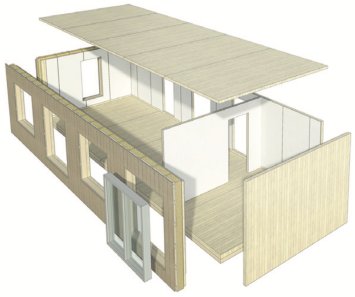

Figure 2.3.2: The different components of a CLT module [19]

The modular structures that result from the use of this technique provide the shortest erection time possible, with a reduction of on-site errors. In counterpart, dimensions are limited by transportation regulations.

Combined with the structural stability of CLT, this makes for a great system especially suited for multi-storey residential buildings, which demand reasonable spans and can accommodate a limited amount of variations between modules. It has furthermore been used for the *Treet* building cited in the introduction, and the *Puukuokka* housing block, which will be presented in Chapter 6. In this way, the designer can combine modular elements like *Lego* blocks to create the building volume.

2.4 Behaviour of CLT structural systems

Thanks to the crosswise arrangement of layers, CLT panels make up for a rigid, dimensionally stable in-plane product suited for walls and floor application. As mentioned earlier, such massive timber product has serious assets to compete not only with other timber structural systems, but also with mineral products like concrete and masonry.

When considering the design of a timber building, several structural systems are conceivable. Timber frames have become popular for low-rise housing projects, and can adopt the same level of prefabrication as CLT. In such construction, walls are typically made of a regularly spaced grid of solid timber studs, framed between horizontal rails. The space between studs allows the fitting of building materials such as insulation or electrical equipment.

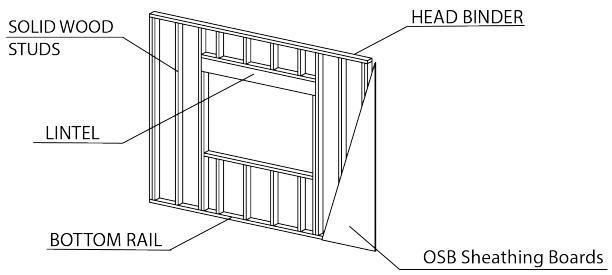

Figure 2.4.1: Typical timber frame wall

As illustrated Figure 2.4.1, two distinct load bearing systems operate in such system: a vertical one, constituted by the timber studs, and a horizontal one via the sheathing. The latter is responsible for the horizontal stiffness of the wall, which greatly limits the number of stories of such construction.

On the other spectrum are massive timber frame structures. Made of massive timber products such as Glued Laminated Timber, the structural system consists in beams and columns, pinned together to form a frame. Once again, additional elements are a must to stabilise the building against horizontal loads. Theses include bracings that can be either made of other timber elements, or steel as it is the case in the White Arkitekter project (cf. Chapter 1).

Structural systems made of CLT, on the other hand, fall into the category of shear walls stabilising systems, which rely on an arrangement of walls to brace a building against horizontal actions. CLT can be its own stabilising system for both vertical and horizontal loads: there is no need for bracing. Shear wall structural systems are very stiff and are commonly used in high-rise buildings, for example with the presence of a core which is one adaptation. Nevertheless, CLT buildings behave very differently from their concrete counterpart. While concrete shear walls act as a rigidly connected unit, such connection is almost impossible to realise in CLT buildings. They are typically connected with steel brackets (to resist shear loads) and hold downs (for tension). The walls are therefore subjected to potential overturning and sliding, in addition to shear and bending deformations.

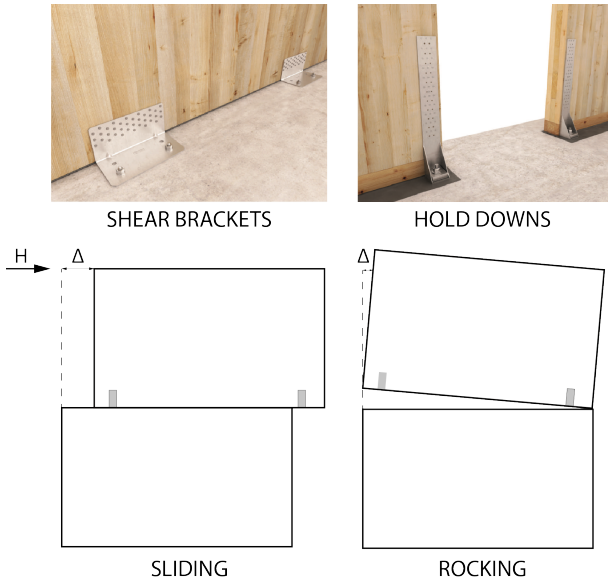

Figure 2.4.2: Typical connections for CLT panels [23] and the deformation they induce

Due to their high in-plane stiffness, CLT walls can be considered rigid when designed for seismic or wind loads [24]. Most deformations occur in the connections, which are designed to prevent brittle failure in the CLT walls by having a lower yield strength. This factor is critical when assessing the stiffness of CLT buildings, and will be discussed in a further section.

Chapter 3

Properties and structural design of CLT

The present chapter derives the material properties of CLT panels, as well as the calculation of their stiffness values. It also introduces the structural assessments that are performed by the framework.

3.1 Characteristic material properties of CLT

As of now, the regulation of CLT properties stays incomplete. Most of its characteristic values are required to be determined through testing, which are described in the standard EN 16351 ([11]), even though the latter gives a few characteristic values without requiring the testing of the panels. A valid model is therefore desired to minimise the amount of testing and prescribe general models to assess a given CLT configuration's performance.

The Graz University of Technology used an approach based on tests as well as a bearing model to present an extensive inventory of CLT properties [25]. The researchers involved work actively towards the integration of CLT in the next revision of the Eurocode 5 [12]. The bearing model follows an idea already used for Glued Laminated Timber (GLT), which consists in determining the material characteristic values from the base material, for instance, the boards or lamellae forming the CLT layers.

The research introduced two CLT strength classes, CL 24 h and CL 28 h, which are used as available CLT grades in this thesis. Their name is inspired by the denomination used for GLT: the number indicating the corresponding bending strength $f_{m,CLT,k}$ (24 or 28) and "h" referring to a homogeneous layup, i.e. made of similar base material. In this case, this grading can be achieved by using lamellae of graded strength T14, having a tensile strength $f_{t,0,l,k}$ of 14 MPa, according to the EN 14080 [26]. The actual difference between them lies in the coefficient of variation $CV[f_{t,0,l}]$ of this tensile strength which itself depends on the grading method [18]. Thus, a $CV[f_{t,0,l}]$ of 25%±5% yields a CL 24 h grade, while the CL 28 h grade can be achieved with a coefficient of variation of 35%±5%. This is reflected in the bearing model equation in bending, which ties the bending strength with the tensile strength of the base material (equation 3.1.1, see below).

The research undertaken at TU Graz led to an exhaustive characterisation of strength and stiffness properties for the two proposed CLT strength classes. Moreover, the researchers also proposed factors relevant to structural design and construction, such as modification factors and partial safety factors, that will be presented in this section.

3.1.1 CLT reference cross section

As for Glued Laminated Timber (GLT), the bearing models developed by TU Graz [25] is valid for an established reference cross section. Variations from this cross section, whether it is in terms of height, number of layers, etc. might be taken into account through modifying factors.

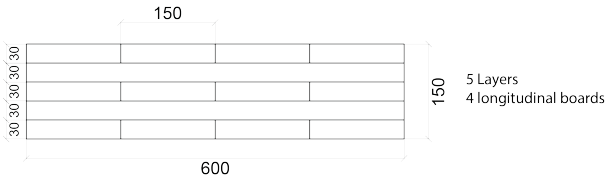

Figure 3.1.1: Reference cross section for CLT (dimensions in mm)

3.1.2 Characteristics defined according to the bearing model

The values exposed here are defined according to the bearing model, meaning that they are derived from the properties of the base material. Therefore, they depend on the layup and composition of the CLT panels.

Bending strength

The bearing model in bending is defined by the Equation 3.1.1:

$$f_{m,CLT,k} = k_{m,CLT} \cdot f_{t,0,l,k}^{0.8} \tag{3.1.1}$$

With

$$k_{m,CLT} = \begin{cases} 3 & \text{for CL24h} \\ 3.5 & \text{for CL28h} \end{cases} \tag{3.1.2}$$

This factor depends on the system strength (i.e. the number of lamellae on the top layer) among others. When the layup has a different overall thickness, it is proposed to adjust the bending strength value by a height factor $k_{h,CLT} = (150/h)^{0.1}$.

Tensile strength parallel to grain

The tensile strength is determined by the equation:

$$f_{t,0,CLT,net,k} = k_{sys,t,0} \cdot f_{t,0,l,k} \tag{3.1.3}$$

With the system strength $k_{sys,t,0}$:

$$k_{sys,t,0} = min \begin{cases} 0.075 \cdot ln(N) + 1 \\ 1.2 \end{cases} \quad \text{for } CV[f_{t,0,l}] = 25\% \pm 5\% \text{ (CL24h)} \tag{3.1.4}$$

$$k_{sys,t,0} = min \begin{cases} 0.130 \cdot ln(N) + 1 \\ 1.35 \end{cases} \quad \text{for } CV[f_{t,0,l}] = 35\% \pm 5\% \text{ (CL28h)} \tag{3.1.5}$$

Compression strength parallel to grain

A bearing model has also been developed for the compression strength parallel to grain. However, Unterwieser and Schickhofer [25] recommends to use the following relation, inspired by the regulation in place for GLT [26]:

$$f_{c,0,CLT,net,k} = f_{m,CLT,k} \tag{3.1.6}$$

Net shear strength in plane

The net shear strength in plane depends on the ratio between the lamellae thickness in the panels weak axis $t_{l,fail}$ [27]:

$$f_{v,net,k} = f_{v,net,k,ref} \cdot min \begin{cases} \left(\frac{40}{t_{l,fail}}\right)^{0.3} \\ 1.20 \end{cases} \tag{3.1.7}$$

With $f_{v,net,k,ref} = 5$ N/mm^2.

Rolling shear strength out of plane

The rolling shear strength $f_{r,CLT,k}$ depends on the ratio between the board width w_l and the layer thickness t_l. A decisive factor of $w_l/t_l = 4$ governs its value; indeed, below this ratio, the rolling shear strength is reduced due to a greater interaction with tensile stress perpendicular to grain [18]. A load bearing model was proposed by [28] taking this value into account:

$$f_{r,CLT,k} = min \begin{cases} 0.2 + 0.3 \cdot \frac{w_l}{t_l} \\ 1.40 \end{cases} \tag{3.1.8}$$

However, this result is not yet regulated by a normative. In the case where the panel is not subjected to testing, the EN 16351 [11] gives conservative values that will be used for the design in this thesis:

$$f_{r,CLT,k} = \begin{cases} 1.1 & \text{if } \frac{w_l}{t_l} \geq 4 \\ 0.7 & \text{otherwise} \end{cases} \tag{3.1.9}$$

Rolling shear modulus

The same study by Erhart [28] proposed a bearing model for the rolling shear modulus of CLT panels:

$$G_{r,CLT,mean} = min \begin{cases} 30 + 17.5 \cdot \frac{w_l}{t_l} \\ 100 \end{cases} \tag{3.1.10}$$

The rolling shear modulus might actually be higher than what is currently regulated. Indeed, it highly relies on the timber ring pattern, and the nature of the boards that are used. For instance, a CLT panel produced with side boards will have a smaller rolling shear modulus than with boards closer to the pith [18].

3.1.3 Characteristics defined by testing or GLT normative

The bearing model is not yet defined for all the strength and stiffness properties. The remaining values are for the moment defined conservatively by testing or inspired by the GLT regulations; they can therefore be applied independently of the layup arrangement. They are summed up in the Table 3.1.1.

Mechanical property		Reference
Tensile strength perpendicular to grain $f_{t,90,CLT,k}$	0.5	[26]
Compression strength perpendicular to grain $f_{c,90,CLT,k}$	3.0	[29]
Torsional shear strength in the glued interface $f_{T,k}$	2.5	[30]
Modulus of elasticity parallel to grain $E_{0,CLT,mean}$	1.05 $E_{0,l,mean}$	[26]
Modulus of elasticity perpendicular to grain $E_{90,CLT,mean}$	300	[26]
Shear modulus (without or with edge bonding) $G_{CLT,mean}$	450 650	[26] [27]
Elastic modulus (5% quantile) $E_{CLT,05}$	5/6 E_{mean}	[26]
Shear modulus (5% quantile) $G_{CLT,05}$	5/6 G_{mean}	[26]
Density $\rho_{CLT,mean}$	$\rho_{l,mean}$	[11]

Table 3.1.1: Mechanical properties of CLT defined by testing or adapted from GLT

3.1.4 Modification factors

Partial safety factor

The traditional partial factors method, as prescribed by the Eurocode 0 [31], requires safety factors to be applied to the characteristic strength to obtain their design values.

For CLT, the safety factor γ_m is proposed to be taken equal to GLT [12], i.e.

$$\gamma_m = 1.25 \tag{3.1.11}$$

Modification factor for duration of load and moisture content

The modification factor k_{mod} is used to describe the influence of load duration and moisture content on strength and stiffness of timber materials.

Each load applied to a timber member is defined according to a load duration class. For example, the structure self-weight is categorised as a permanent action, while a variable action such as the wind can be either instantaneous or short-term [12].

The other influencing factor is the service class, which reflects the moisture content to which the element is subjected. For CLT, only service classes 1 and 2 are allowed [11]; the first one corresponding to a lower moisture content than the second (see Eurocode 5, Section 2.3.1.3 [12]). For these classes, the k_{mod} factor is not affected.

From these parameters, the modification factor k_{mod} can be determined from the Table 3.1.2 [25]:

	Service class	Load duration class				
		Permanent	Long term	Medium	Short term	Instantaneous
k_{mod}	1 or 2	0.6	0.7	0.8	0.9	1.1

Table 3.1.2: Values of the modification factor for load duration and moisture content k_{mod}

When several loads from different categories are acting together, the value of k_{mod} must correspond to the shortest action [12].

Deformation factor

The deformation factor k_{def} is introduced in the Eurocode 5 [12] to take creep into account, since timber in general is subjected to this phenomenon. Once again, this factor depends on the service class, but also on the layup configuration. Thus, k_{def} must be increased by 10% when applied on a CLT panel of less than 7 layers. The Table 3.1.3 lists the values for k_{def} according to these parameters [25].

	Layers	Service class	
		1	2
k_{def}	> 7	0.8	1
	≤ 7	0.85	1.1

Table 3.1.3: Values of the deformation factor k_{def}

3.2 Design values for CLT

The safety factor γ_m and the modification factors k_{mod} and k_{def} defined in Section 3.1.4 have an impact on the design strength and stiffness values, that are to be compared to the actions values [12].

For a given strength value, its design counterpart is given by the equation:

$$X_d = \frac{k_{mod} \cdot X_k}{\gamma_m} \tag{3.2.1}$$

The stiffness properties, however, are not reduced by the load duration factor, as shown in this example for the design Young Modulus E_d:

$$E_{mean,d} = \frac{E_{mean}}{\gamma_m} \tag{3.2.2}$$

Finally, the deformation factor intervenes for the deflection calculations in the quasi-permanent combination (SLS, Framework Manual Equation 4.20). When calculating a stiffness property, for instance the bending stiffness (EI), one must reduce the corresponding modulus accordingly (example given on E_{mean}):

$$E_{mean,fin,d} = \frac{E_{mean,d}}{1 + k_{def}} \tag{3.2.3}$$

3.3 Stiffness values

The stiffness values define the orthotropic behaviour of CLT panels. In this project, they will be used to define the equivalent isotropic modelling, as well as the orthotropic stiffness matrix for the simulations presented in Chapter 5.

3.3.1 Bending stiffness out-of-plane

Several methods can be used when it comes to estimating the bending stiffness of a CLT panel for loads out-of-plane. The bending stiffness characterise the bending deflections out-of-plane; in this project, this concerns the design of CLT floors, which will be attributed an equivalent Young modulus based on this value (cf. Chapter 5).

The most accurate method to describe the strength and bending properties of CLT is the Shear Analogy Method, developed by Kreuzinger (cited in [17]), which accounts for both bending and shear deformation. This method requires the use of a plane frame analysis program and might therefore not be suitable in the frame of this thesis, but its details are explained in [17].

The composite theory, detailed in [32], is inspired by the calculation method to evaluate the bending stiffness of plywood. To account for the strength and stiffness properties of each layer (both parallel and crosswise), composition factors are applied which depend on the loading and the layup of the CLT panel. However, this method does not take the shear deformation into account. The latter becoming significant when the span-to-depth ratio l/h decreases, due to a low rolling shear modulus, the composite method shall not be used for $l/h \leq 30$.

Finally, another approach uses the mechanically jointed beams procedure from the Annex B of the Eurocode 5 [12], and is called the γ-method. The CLT in bending is considered as several boards in the longitudinal direction, joined by the crosswise layers. The computed effective bending stiffness K_{CLT} is therefore the result of the area moment of inertia of the longitudinal plies, connected with mechanical fasteners with a connection efficiency factor γ, between 0 (no connection) and 1 (fully rigid):

$$K_{CLT} = \sum E_i \cdot I_i + \sum \gamma_i \cdot E_i \cdot A_i \cdot e_i^2 \tag{3.3.1}$$

Where e_i is the distance between the layer centre of gravity and the one of the whole cross section. The longitudinal layers are given the mean modulus of elasticity parallel to the grain $E_{0,CLT,mean}$, and the cross layers the mean modulus of elasticity perpendicular to the grain $E_{90,CLT,mean}$.

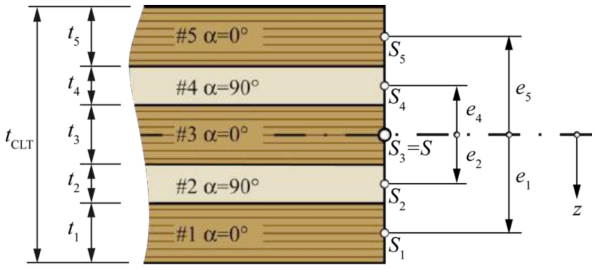

Figure 3.3.1: Parameters for the estimation of a CLT panel's bending stiffness

Technically, the γ factor should reflect the deformability of the cross layers, i.e. their rolling shear stiffness. However, in practice, the glued interface can be considered as fully rigid, i.e. $\gamma = 1$. Moreover, the ratio between $E_{0,CLT,mean}$ and $E_{90,CLT,mean}$ being high (≈ 30), the contribution of the cross layers can be ignored [33].

This method predicts the deflection out-of-plane with sufficient accuracy in the practical range of $l/h \geq 15$ and will therefore be used to estimate the bending stiffness of CLT elements in this thesis.

3.3.2 Shear stiffness out-of-plane

The shear stiffness of a CLT element loaded out-of-plane is based on the shear stiffness of a rigid composite beam, modified by a shear correction factor κ [33]. It characterises the shear component of out-of-plane deflection, and will be used in the framework to add this contribution to the total deflection of slabs.

$$S_{CLT} = \kappa \cdot \sum G_i \cdot A_i \tag{3.3.2}$$

Where A_i is the cross sectional area of the layer i; $G_{CLT,mean}$ is used for longitudinal layers and $G_{r,CLT,mean}$ is used for cross layers.

The shear coefficient factor κ has been analitically determined for different layups, depending on the ratio between the thickness of longitudinal layers t_0 and the gross thickness t_{CLT} [33].

For practical calculations, in the frame of this thesis, we will estimate κ at $1/3$ of the shear coefficient factor for a unidirectional rectangular cross section (0.83) [18]: $\kappa = 0.28$.

3.3.3 Axial stiffness

To estimate the flexural deformation of CLT panels under in-plane loads, such as the wind action on floors or axial loads on walls, the axial stiffness is computed in two directions. This will influence, notably, the horizontal load distribution between walls, and the building sway. Once again, only the layers oriented according to the corresponding direction are taken into account [33]:

$$D_x = E_{0,CLT,mean} \cdot \sum t_{i,x} \tag{3.3.3}$$

$$D_y = E_{0,CLT,mean} \cdot \sum t_{i,y} \tag{3.3.4}$$

These values are used to propose and equivalent elasticity modulus for walls, see Chapter 5.

3.3.4 Shear stiffness in-plane

The shear deformation caused by in-plane loads is linked to the shear stiffness of the CLT plate:

$$S_{xy} = G^* \cdot t_{CLT} \tag{3.3.5}$$

The effective shear modulus accounts for the two mechanisms in action in a CLT element subjected to in-plane shear, namely a shear deformation and a torsional deformation. The solution has been adjusted with a factor α_T through FE modelling in [34]:

$$G^* = \frac{G_{CLT,mean}}{1 + 6 \cdot \alpha_T \cdot \left(\frac{t_l}{w_l}\right)^2} \text{ with } \alpha_T = 0.32 \cdot \left(\frac{t_l}{w_l}\right)^{-0.77} \tag{3.3.6}$$

While it is not possible to consider this value for an isotropic modelling, it will be used to define the orthotropic material and its influence will be investigated.

3.3.5 Twisting stiffness

The twisting stiffness of a CLT panel characterises the deformation of panels subjects to opposite out-of-plane loads. While this is not considered in the proposed approach, its value is necessary to establish the orthotropic stiffness matrix of CLT products, developed in Chapter 5. For this reason, it is proposed to follow the guidance used by the manufacturer Stora Enso [35] and to use a simplified calculation:

$$K_{xy} = K_{twist} \cdot G_{0,mean} \cdot \frac{t^3}{12} \tag{3.3.7}$$

Where $K_{twist} = 0.65$ (constant) and t is the thickness of the CLT cross section.

3.4 Structural verification of CLT panels

3.4.1 Design of CLT walls subjected to in-plane loading

The section deals with the strength design of CLT panels used as walls, subjected to tension, compression and shear forces in plane. All of the safety checks presented below have been implemented in the framework via the *Wall Design*, presented in Chapter 4 and in the Framework Manual, Section 6.3.

Tension and Compression

The check performed for axial loads such as tension and compression is carried out under the assumption that the elasticity modulus $E_{0,mean}$ is the same for all layers. Only the effective area of layers $A_{net,0} = \sum_i t_{i,0}$ with their grain parallel to the load is considered. The following criteria must be satisfied:

$$\frac{N_d}{A_{net,0}} \leq f_{t,0,CLT,net,d} \tag{3.4.1}$$

Where N_d is the design tension force.

The verification of CLT panels under compression is roughly similar, in that way that the same effective area is considered. However, the member slenderness must be considered against potential buckling. The design proposed by [33] follows the procedure from the Eurocode 5 [12], with a modified relative slenderness ratio λ_{rel}:

$$\lambda_{rel} = \sqrt{\frac{A_{net,0} \cdot f_{c,0,CLT,net,k}}{n_{cr}}} \tag{3.4.2}$$

Where n_{cr} is the ideal elastic buckling load:

$$n_{cr} = \frac{K_{CLT,05} \cdot \pi^2}{l_k^2 + \frac{K_{CLT,05}}{S_{CLT,05}}} \tag{3.4.3}$$

l_k being the wall's buckling length, $K_{CLT,05} = 5/6 \cdot K_{CLT}$ and $S_{CLT,05} = 5/6 \cdot S_{CLT}$ obtained from equations 3.3.1 and 3.3.2 by replacing the moduli by the 5% quantiles values.

The relative slenderness ratio can then be replaced in the Eurocode 5 calculations, and the obtention of the reducing factor k_c for buckling proceeds as follow:

$$k = 0.5 \cdot (1 + \beta_c \cdot (\lambda_{rel} - 0.3) + \lambda rel^2) \tag{3.4.4}$$

$$k_c = \frac{1}{k + \sqrt{k^2 - \lambda_{rel}^2}} \tag{3.4.5}$$

β_c, depending of the production quality, is the straightness factor and is proposed to be equal to that of GLT, i.e. 0.1.

The criteria that must be satisfied is thus:

$$\frac{N_d}{k_c \cdot A_{net,0}} \leq f_{c,0,CLT,net,d} \tag{3.4.6}$$

Shear in plane

As CLT walls will likely be used as a stabilising system, they have to resist the shear forces from horizontal loads such as wind or earthquakes. When subjected to shear loads, CLT panels can experience two main failure mechanisms [30]:

- shear failure in the layers
- torsion failure at the glued interface

Both mechanisms must be checked accordingly. Bogensperger [30] proposes to decompose the CLT element in representative volume elements (RVE) and representative volume sub-elements (RVSE) to determine the corresponding stresses from a given design shear force $n_{xy,d}$ in kN/m.

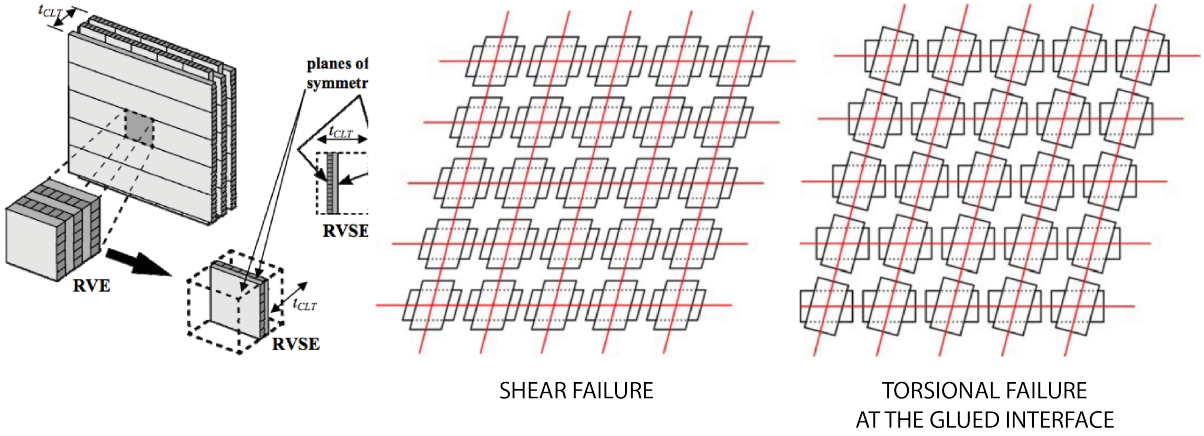

Figure 3.4.1: Definition of RVE and RVSE (left), shear failure mechanism (middle) and torsional failure mechanism (right) [30]

Each layer of the RVSE has an ideal thickness t_i^* determined as follow:

$$t_i^* = \begin{cases} min(2 \cdot t_i; t_{i+1}) & \text{for an outer layer} \\ min(t_i; t_{i+1}) & \text{for an inner layer} \end{cases} \tag{3.4.7}$$

The overall thickness of the RVSE is:

$$t^* = min\left(\sum_{1}^{n-1} t_i^*; t_{CLT}\right) \tag{3.4.8}$$

On this basis, the proportionate shear force in a n-layer CLT RVSE is:

$$n_{xy,RVSE(i)}^* = \frac{n_{xy}}{t^*} \cdot t_i^* \tag{3.4.9}$$

Each RVSE is therefore subjected to a constant nominal design shear stress:

$$\tau_{0,d} = \frac{n_{xy,d}}{t^*} \tag{3.4.10}$$

For the first mechanism (shear), the effective shear stress of a RVSE is:

$$\tau_{v,d} = 2 \cdot \tau_{0,d} \leq f_{v,CLT,d} \tag{3.4.11}$$

The second mechanism (torsion in the glued interface) produces a design torsional stress given by the equation:

$$\tau_{T,d} = 3 \cdot \tau_{0,d} \cdot \frac{t_l}{w_l} \leq f_{T,d} \tag{3.4.12}$$

3.4.2 Design of CLT floors subjected to out-of-plane loading

In the approach proposed in the frame of the thesis, the CLT floors are designed for out-of-plane loads for bending and shear strength, as well a vertical deflection. The checks presented in this section have been implemented with the *Slab design* component, see next chapter and the Framework Manual section 6.4.

Bending out-of-plane

When subjected to out-of-plane loads, a bending stress develops in the CLT cross section. A linear stress distribution is assumed over the hypothesis that the cross section remains plane upon deformation. However, due to possible gaps or cracks between layers, the axial stresses cannot always be transferred in the cross layers [33]. The modulus of elasticity of the cross layers $E_{90,CLT,mean}$ can thus be taken as 0; this increases the stress in the longitudinal layers, giving a conservative design. The stress distribution in the cross section is the following:

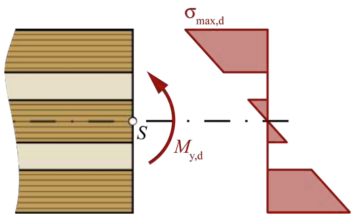

Figure 3.4.2: Bending stress distribution over the CLT cross section [33]

The maximum design bending stress occurs in the outer layer, and must be checked against the design bending strength of the panel:

$$\sigma_{m,max,d} = \frac{M_d}{K_{CLT}} \cdot \frac{t_{CLT}}{2} \cdot E_{0,CLT,mean} \leq f_{m,CLT,d} \tag{3.4.13}$$

Where M_d is the design bending moment in the cross section.

Transverse shear

Along with bending stresses, transverse shear forces also develop in slabs, and reach their maximum at the supports; this effort results from the variation of the bending moment over the thickness. Similarly to the bending stresses, the transverse shear force develops over each layer with the following equation, reduced to a 1m length:

$$\tau_0(z) = \frac{V_z \cdot \int_0^{z_0} E(z) \cdot z \cdot dz}{K_{CLT}} \tag{3.4.14}$$

Where V_z is the transverse shear force acting on the section.

Once again, assuming that the young modulus of cross layers $E_{90,CLT,mean}$ is negligible, the variation of the shear stresses over cross layers is null, which leads to the following shear stress profile:

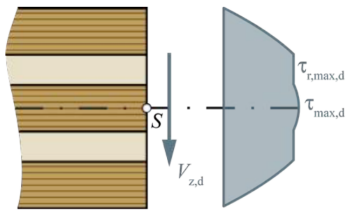

Figure 3.4.3: Shear stress distribution over the CLT cross section [33]

Due to the cross-wise arrangement, the parallel layers will be subjected to shear stresses, while the crosswise layers must resist rolling shear stresses. The maximum shear/rolling shear stresses occur at the middle and second to middle layers, and must satisfy:

$$\begin{cases} \tau_{max,d} \leq f_{v,net,d} \text{ for parallel layers} \\ \tau_{r,max,d} \leq f_{r,d} \text{ for crosswise layers} \end{cases} \tag{3.4.15}$$

This setup will be taken into account in the structural verifications carried out by the design framework.

Chapter 4

Parametric Framework

This chapter presents the principles of the framework developed as part of this thesis. It states its objectives, as well as the underlying assumptions and limitations that ensue.

4.1 Method

4.1.1 Objectives

Cross Laminated Timber, given its relative novelty, suffers from little integration in the design workflow: the methods currently in use to design buildings relying on CLT structural systems either require an important knowledge in Finite Element Modelling (FEM), or in structural analysis in general. Such requirements are likely to result in the situation where engineers act as assistants to the building designer. In this configuration, geometric and calculation models are separated, thus increasing the risk of divergences and providing no direct feedback on design modifications [13]. This process can become cumbersome especially in the early design stages, where multiple solutions are evaluated.

Hence, the method which is proposed in this thesis aims at bridging the gap between design and structural performance, by combining them within a single environment. It develops an approach to the structural design of buildings with Cross Laminated Timber, relying on the considerations presented in Chapter 3.

The approach is conceived to accommodate the needs of designers who might not possess a deep expertise in CLT or structural design, by providing quasi-instantaneous feedback to guide them through the evaluation of several design alternatives. In return, the expertise embedded within the framework aspires to broaden their knowledge and give them the keys to achieve a sensible, informed and integrated structural accommodation.

The method wishes itself to be highly flexible, in order to embrace the multiple iterations characteristic from the early stages of the design.

4.1.2 Developed environment

In order to develop the framework, the approach consists in using a geometry modelling software and a Finite Element Analysis (FEA) software, linked by a visual programming interface. This setting

allows the combination of geometric and calculation models into an integrated dynamic model [36], which share information in both directions.

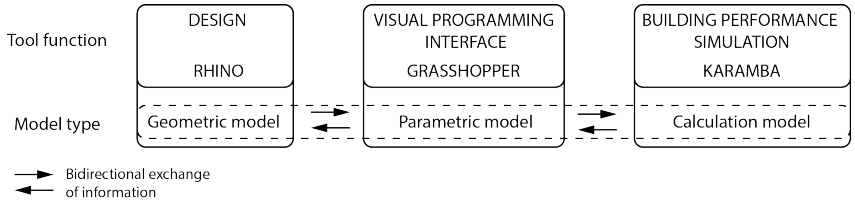

Figure 4.1.1: Integrated dynamic model, adapted from Negendahl [36]

This first role is fulfilled by Rhino. Developed by McNeel & Associates, this software is a free form surface modeller based on NURBS curves. It gives the ability to generate any kind of geometry, and has become popular among designer for non-standard objects. Moreover, it offers communication with several external software, which widens the range of applicability in the construction field ([37]). However, in the developed framework, Rhino is only used, optionally, as primary input for the design and as a visual platform. Most of the data is handled by the visual programming interface provided by Grasshopper.

Grasshopper is a graphical algorithm editor developed by David Rutten, within McNeel & Associates. Using a visual programming language (VPL), designers can explore generative design solution without the need for an extended knowledge in programming. It is fully embedded in the Rhino modeller and is able to exploit its graphical capabilities, while providing a broad range of additional plug-ins by third-party developers.

Among them, we will be mostly interested in Karamba [38]. This parametric structural engineering tool is developed by Clemens Preisinger and Bollinger-Grohmann-Schneider. It features a wide set of tools to perform FE Analysis for buildings, using notably shell elements. Karamba is integrated to Grasshopper, and uses the visual programming language of this environment.

Finally, an additional layer is added to the overall workflow through MS Excel, to simplify the handling of an important amount of data. The communication between the two software is made with the Grasshopper plug-in GhExcel.

4.2 Framework

4.2.1 Overview

The proposed framework adopts this parametric design philosophy, and combines the flexibility of such an environment with the design of mass customised CLT buildings; it aims towards a streamlined workflow to lead the designer from the building's geometry to relevant information about its structural performance.

As most processes in the design field, the building conception starts with a geometry. Whether it is at an advanced stage, where decisions are largely fixed, or at a more conceptual one, the first phase of the framework consists in modelling the arrangement of the space which represents the project. This step includes the definition of a floor layout and, for example, basic parameters such as the number of stories and the height.

The way these decisions are made can reflect the state of advancement of the design: one can take advantage of the parametric environment to generate several proposals before settling down for one option.

However, the novelty resides in the concept of model population and mass customisation. After defining the primary outlay, the designer can, at will, generate new geometry and build up a whole concept on a minimal amount of basic models.

The next step consists in integrating the CLT structural design as presented in Chapter 2. Through layup definition, the CLT material is applied to given elements; the model is then ready for the structural analysis, after a preparation phase, which yields a wide range of outputs.

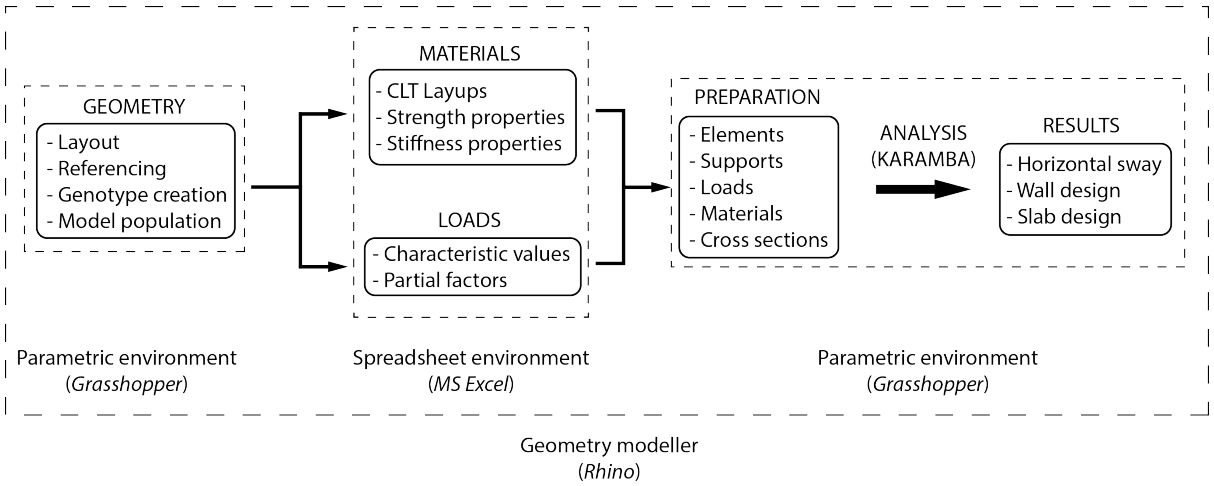

Figure 4.2.1: Framework implementation workflow

The geometry input is very important, and is where the user can express all his creativity. The following steps, however, are meant to inform him/her with relevant feedback and provide help to guide his/her decision. The framework is thus an iterative process: the designer controls the geometry and simultaneously sees the impact of its modification.

For each of these steps, macro-modules have been developed in the VPL. The objective is to make the transition between steps seamless by requesting as less inputs as possible, and suppress the barrier between the design concept and the structural design: once the full setup is in place, instant communication between them is established. They cover all the required steps as illustrated in the Figure 4.2.1, from the creation of the geometry, to the load and material definition, the preparation for the structural analysis in Karamba, and the obtention of the structural results. The details of their functions and use is explained in the second book of this thesis, the "Framework Manual". The Chapter 6, on the other hand, illustrates a wide range of available structural feedback, applied to the Puukuokka case study.

4.2.2 Conceptual approach

Mass customisation is introduced at an assembly scale by offering the opportunity to the users to define their own CLT product, through the control of layer thicknesses, their number and arrangement [39]. The designers can therefore free themselves from proprietary products, and propose their own design solution.

Inspired by the prefabrication and modular building systems presented in Section 2.3, the framework also introduces the concept of genotypes and phenotypes [39].

In biology, the genotype is a part of the DNA which defines a set of general characteristics. A phenotype, on the other end, is produced by a genotype put into context, shaped by the environment

and reflects the actual characteristics of an individual. Applied to prefabricated products within the framework, a genotype represents a family of CLT elements, defined by a general geometry and layup. This genotype is then adapted to a given location in the building to fulfil its function, whether it is a wall or a floor. While its shape might vary due to environmental constraints, the resulting phenotype, or instance, inherits its global characteristics from its parent.

The design which results is therefore characterised by a repetition of elements sharing similar properties and geometries, which gain their individuality when placed in the context of the building. These properties are left entirely up to the designer, within the boundaries of CLT's technical requirements.

4.3 General structural assumptions for the model

The structural representation that comes out of this approach obeys to certain modelling choices that have an influence on the results.

For a start, the software proposes only shell elements. Such modelling reproduces the behaviour of panels subjected to in-plane membrane forces as well as out-of-plane bending moment. This is suitable to characterise the elements that are part of the model. However, the use of shell elements might have an effect on the resulting lateral load repartition. When evaluating this parameter, floors can either be considered as flexible or rigid. In the first case, the shear force transferred to a given shear wall can be calculated according to the tributary area method. For example, a slab supported by two shear walls will distribute half of the shear force to each shear wall, independently of their stiffness. On the other hand, if the floor is considered to act as a rigid diaphragm, the force distribution is made according to the relative stiffness of each wall. CLT floors are usually modelled as rigid diaphragms, upon the assumption that the panels that compose them are properly fastened between each other [17]. Therefore, by using shell elements, the lateral load distribution might be different from what could be expected from the former type of modelling. However, the stiffness of CLT floor shell elements should in practice be high enough for them to act as if rigid.

Another important modelling choice comes in the connections between CLT walls and floors. Unless releases between elements are specified, the connections are assumed rigid. This is not the case in CLT buildings, where slabs are hinged. Furthermore, CLT elements used as floors generally behave as one-way slabs, spanning along their main direction. The "weak" direction therefore mainly transfers shear forces to counteract the horizontal loads. This means that the deflection resulting from the Karamba analysis will likely be underestimated, since they assume a slab rigidly connected along its four edges.

On the other hand, this connection model also has an important impact on the building's horizontal deflection, since each piece of wall is rigidly connected to the one below and above. In reality, the connections are made by shear brackets and hold downs. When subjected to horizontal actions such as seismic or wind loads, the CLT walls are subjected to four different deformations (as explained in Section 2.4), and an important contribution comes from the connections. Therefore, assuming rigid connections between the walls might limit the validity of the results.

4.4 Structural design methodology

Among the multiple components developed in the parametric environment (cf. Framework Manual), three are devised to perform the structural analysis of CLT buildings and provide feedback to the

users. The methodology behind these components will be explained in this section; the details of how to operate each component is explained in the Framework Manual.

The first component aims at the assessment of the building's horizontal sway. This component relies mostly on the *Nodal Displacements* component from Karamba [40] which provides the displacements of every single node of the model. The *Horizontal Sway* component that has been developed retrieves a highest point on the building and its corresponding displacement, and combine them with the factors to obtain the displacement for each load combination (cf. Framework Manual, Section 4.6). The horizontal displacement that results is the absolute distance along the two horizontal axes, x and y. The knowledge use from Chapter 3 is here limited to the definition of equivalent elasticity modulus for floors and walls, based respectively on the bending stiffness out-of-plane and the axial stiffness, as explained Chapter 5.

The *Wall Design* component, as its name indicates, performs the structural verification of walls under in-plane loads. It provides outputs for the support reactions, as well as compression, tension, shear and torsional shear stresses. The support reactions are simply obtained from the selection of values for corresponding supports as provided by the Karamba *Reaction Forces* component [40]. The 4 last results however rely on the theory detailed in Section 3.4.1.
For the tension and compression check, the vertical forces n_{yy} (local y direction) are at first retrieved from the *Shell Forces* component from Karamba and combined with the load combination factors. The tension and compression stresses are then computed by dividing these forces by the effective thickness (effective area for 1m length) as explained in Section 3.4.1. Negative (compression) and positive (tension) values are then dispatched and compared with the respective strength value of the CLT layup. An additional step is performed for the compression stresses by including the calculation of the buckling factor k_c.
Shear and torsional stresses are derived from the in-plane shear forces n_{xy} as calculated from the same Karamba component. After the load combinations, these forces are processed according to the methodology from Section 3.4.1 and compared to the respective shear and torsional strength of the CLT panel.

The final component, *Slab Design*, is particular in itself since creating a sub-model detached from the rest of the building. Reasons for this choice are explained in Section 5.3.1. Beyond this, results are delivered for the deflection out-of-plane, bending, shear and rolling shear stresses as presented in Section 3.4.2. The calculation of the out-of-plane deflection is provided by the "Displacement" output of the Karamba *Analyze Th. I* and processed into the several load combinations. The contribution from shear at mid span is added based on the shear stiffness out-of-plane of the CLT floor, calculated according to Section 3.3.2.
The obtention of the design stresses are based on the moment out-of-plane m_{yy} and the transverse shear force v_{yy} from the *Shell Forces* from Karamba, for bending and transverse shear respectively. The calculation of bending stresses follows the method presented in Section 3.4.2 to present the maximum bending stress in the bottom outer layer of the CLT, from the moment out-of-plane.
Shear and rolling shear stresses are based on the transverse shear forces following the theory presented in Section 3.4.2. The two design values that are provided are stresses existing in the middle and second-to-middle layers. Depending on the layup, these layers will be subjected either to shear or rolling shear stresses, depending on their orientation (0° or 90° respectively); this detail is reflected in the textual output.

4.5 Use and limitations

4.5.1 Applicable cases

The framework allows the verification of buildings featuring a structural system made of CLT panels. It is suited best for concepts with a fairly simple geometry, where a small number of products are adapted in a larger scale; for instance, low to mid-rise buildings with identical storeys.

Indeed, some limitations occur in the load application, presented in the Framework Manual Section 4. For instance, the wind load calculation as prescribed by the Eurocode 1-4 [41] is in theory only applicable to rectangular buildings. For geometries varying drastically from this simple case, it is recommended to proceed to an advanced wind analysis, especially in the case of high-rises. Moreover, the snow loads are limited by the roof types described in the Eurocode 1-3 [42].

4.5.2 Range of structural feedback

The information is delivered for the design of CLT panels used as floors subjected to out-of-plane loading. It can be used to check their design for bending and transverse shear in the Ultimate Limit State (ULS, see Framework Manual Section 4.6), as well as vertical deflection in the Serviceability Limit State (SLS, see Framework Manual Section 4.6). However, floors are subjected to other design criteria: their axial strength must be checked for shear from the wind load, as well as in-plane moments. Furthermore, vibrations also play an important role and is disregarded in this research.

As far as the design of CLT walls is concerned, they are only checked for in-plane stresses (axial and shear). In a fully operational structural analysis, one would need to evaluate the moments out-of-plane, for example.

Finally, structural fire safety is not included in this research.

4.5.3 Isotropic modelling of CLT panels

Cross Laminated Timber is a multi-layered composite material, and its accurate modelling is complex. As a simplified approach, an orthotropic characterisation is generally used; unfortunately, the design of such materials is not yet available in Karamba. Therefore, an equivalent isotropic modelling is suggested and its validity will be evaluated in Chapter 5.

Chapter 5

Orthotropic and Isotropic Modelling

Cross Laminated Timber is best described with orthotropic properties. However, due to software limitations, an equivalent isotropic modelling is proposed. Both approach are presented and their differences are investigated in this chapter.

5.1 Orthotropic modelling of CLT elements

Due to its complexity, FE modelling of CLT panels might prove to be complex. Several possibilities can be adopted when representing the CLT panels with FEM. The most exact solution consists in generating a detailed 3D FE model representing each layer of the configuration, and assign them orthotropic properties. The layers are then connected to each other by contact elements with a frictional coefficient reflecting that of the glued interface, which might be either rigid or flexible ([43]). Another proposal suggests using 2D shell elements connected with non-linear springs, that represent "the effects of rolling shear and bonding of the interface" ([44]).

However, this multi-layered approach requires an advanced mastering, and does not seem suitable for a large scale design of CLT panels. Moreover, most common FEM software does not offer this possibility. Instead, an equivalent single-layer orthotropic material can be used, by defining a stiffness matrix in the chosen software ([35]). This matrix reflects the Hooke's Law for the orthotropic CLT, using the different stiffness values calculated in Section 3.3:

$$\begin{Bmatrix} m_x \\ m_y \\ m_{xy} \\ v_x \\ v_y \\ n_x \\ n_y \\ n_{xy} \end{Bmatrix} = \begin{bmatrix} K_{CLT,x} & & & & & & & & \\ & K_{CLT,y} & & & & & & & \\ & & D_{xy} & & & & & & \\ & & & S_{CLT,x} & & & & & \\ & & & & S_{CLT,y} & & & & \\ & & & & & D_x & & & \\ & & & & & & D_y & & \\ & & & & & & & S_{xy} & \end{bmatrix} \cdot \begin{Bmatrix} \kappa_x \\ \kappa_y \\ \kappa_{xy} \\ \gamma_x \\ \gamma_y \\ \epsilon_x \\ \epsilon_y \\ \gamma_{xy} \end{Bmatrix} \tag{5.1.1}$$

The stiffness matrix is diagonal, and each term outside the diagonal are equal to 0; they are very small and can be neglected. Moreover, the assumption is made that the CLT panel is not edge glued ([35]). In that case, stresses do not transfer between adjacent lamellae: the Poisson ratio can be taken as $\nu = 0$, resulting in the nullity of the remaining coefficients.

Once generated, the matrix can be used to manually define an orthotropic plate material that will be attributed to the CLT panels in the FE model.

As seen previously, the stiffness values of a CLT panel depends on the geometry of the laminate. For this reason, one different stiffness matrix is needed for each type of CLT. This characterisation of the CLT material will be used in a Section 5.3 as a reference, to assess the proposed method validity.

For simplification, the notations $KCLT, x$, $K_{CLT,y}$, $S_{CLT,x}$ and $S_{CLT,y}$ will be referred to as K_x, K_y, S_x and S_y respectively for the remaining of this report.

5.2 Proposed isotropic modelling

As explained in Section 4.5, it is not possible to define an orthotropic material in Karamba. Therefore, a isotropic material that recreates this behaviour must be suggested. Such simplification has already been made by Tolszczuk-Leclerc [45], but only took the bending behaviour into account. In this research, shear and axial forces are also part of the structural design approach.

For an isotropic plate, the stiffness matrix defined in Section 5.1 takes the following shape:

$$\begin{Bmatrix} m_x \\ m_y \\ m_{xy} \\ v_x \\ v_y \\ n_x \\ n_y \\ n_{xy} \end{Bmatrix} = \begin{bmatrix} D & \nu D & & & & & & \\ \nu D & D & & & & & & \\ & & D(1-\nu) & & & & & \\ & & & Gt & & & & \\ & & & & Gt & & & \\ & & & & & \frac{E\cdot t}{1-\nu^2} & \frac{E\nu t}{1-\nu^2} & \\ & & & & & \frac{E\nu t}{1-\nu^2} & \frac{E\cdot t}{1-\nu^2} & \\ & & & & & & & Gt \end{bmatrix} \cdot \begin{Bmatrix} \kappa_x \\ \kappa_y \\ \kappa_{xy} \\ \gamma_x \\ \gamma_y \\ \epsilon_x \\ \epsilon_y \\ \gamma_{xy} \end{Bmatrix} \tag{5.2.1}$$

Where t is the plate thickness, E is the Young Modulus of the material, ν its Poisson ratio, $G = \frac{E}{2(1+\nu)}$ the Shear Modulus, and $D = \frac{Et^3}{12(1-\nu^2)}$ the bending and axial stiffness of the plate.

The entire behaviour of the isotropic plate is dictated by only two parameters (E and ν), against 8 in the orthotropic stiffness matrix: it is therefore impossible to find an equivalence between them. However, the stiffness matrix suggested for CLT ([35]) is diagonal: the resulting efforts are independent from each other, due to a Poisson ratio $\nu = 0$. Inspired by this example, it is proposed to assign a Poisson ratio $\nu = 0$ to the isotropic representation of CLT.

The previous matrix then becomes:

$$\begin{Bmatrix} m_x \\ m_y \\ m_{xy} \\ v_x \\ v_y \\ n_x \\ n_y \\ n_{xy} \end{Bmatrix} = \begin{bmatrix} EI & & & & & & & \\ & EI & & & & & & \\ & & EI & & & & & \\ & & & \frac{Et}{2} & & & & \\ & & & & \frac{Et}{2} & & & \\ & & & & & Et & & \\ & & & & & & Et & \\ & & & & & & & \frac{Et}{2} \end{bmatrix} \cdot \begin{Bmatrix} \kappa_x \\ \kappa_y \\ \kappa_{xy} \\ \gamma_x \\ \gamma_y \\ \epsilon_x \\ \epsilon_y \\ \gamma_{xy} \end{Bmatrix} \tag{5.2.2}$$

Where I is the area moment of inertia of the plate.

5.2.1 Isotropic stiffness properties for CLT walls

In this framework, it is of interest to determine the axial and shear forces in the wall elements.

In the orthotropic modelling of the CLT walls, the axial forces in the z direction will be expressed as:

$$n_x = D_x \cdot \epsilon_x \tag{5.2.3}$$

By assigning a Young Modulus $E_{eq,IP} = \frac{D_x}{t}$, the value of the axial forces in the walls should be left unchanged. The nullity of the Poisson ratio is ensured by defining the shear modulus as $G_{eq,IP} = \frac{E_{eq,IP}}{2}$.

The proposal also conserves the relative stiffness values between the different walls; consequently, the lateral loads are distributed as it would be in the orthotropic model.

5.2.2 Isotropic stiffness properties for CLT floors

CLT floors are checked for bending moments, shear forces and vertical deflection.

The definition of an equivalent out-of-plane Young Modulus is based on the orthotropic bending stiffness in the main direction:

$$E_{eq,OP} = \frac{K_x}{I} \tag{5.2.4}$$

With $I = \frac{t^3}{12}$. The shear modulus is defined once again as $G_{eq,OP} = \frac{E_{eq,OP}}{2}$.

With this setup, the bending moment and vertical deflection can be approximated. Moreover, the Young Modulus should be high enough to ensure a similar in-plane behaviour of the floor and transfer the loads accordingly.

5.3 Validity of the approach

In order to study the influence of such material definition on the results, reference models are setup for both an orthotropic definition of CLT and an isotropic one, using the software Robot Structural Analysis (Autodesk). Various parameters and elements are evaluated.

5.3.1 Results on Floors

Setup and material definition

It is proposed to study the discrepancy between the orthotropic and isotropic model against the length to width ratio l/w of the slab. Indeed, a plate with a l/w ratio higher than 2 is usually said to act as a one-way slab; calculations can therefore be done as for a beam. On the other hand, for a ratio lower than 2, the plate acts as a 2-way slab.

The accuracy of the isotropic model is examined in terms of vertical deflection, bending moments and transverse shear force. These values are evaluated for an orthotropic and isotropic plate, simply

supported on its four edges; a vertical load of $q = 5$ kN/m^2 is applied, the self-weight of the structure is ignored. Tests are carried out for l/w ratios from 1 to 8. The width w of the plate is set to 4m to ensure an adequate span-to-depth ratio ($l/t \approx 27$, see Section 3.3.1); its length l therefore varies from 4 to 32m. The orthotropic direction is set along the width of the plate.

All of the tests are realised with the modelling of a 150mm thick CLT panel showing the characteristics presented in Figure 5.3.1.

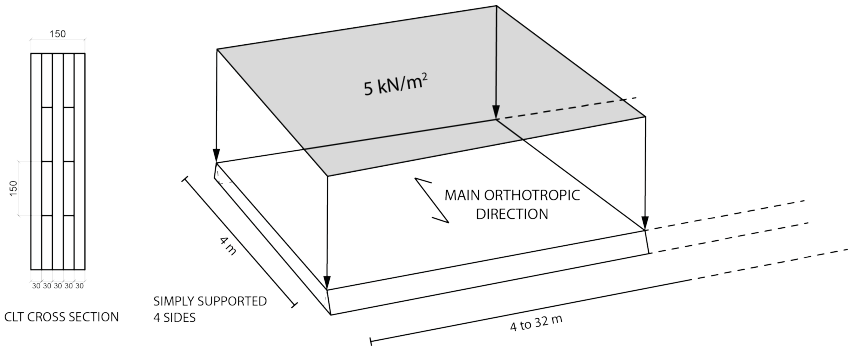

Figure 5.3.1: Cross section for the orthotropic CLT slab and simulation setup

The orthotropic model is characterised by the definition of the orthotropic stiffness matrix for the above cross-section (see Equation 5.1.1), i.e.:

$$\boldsymbol{K} = \begin{bmatrix} 2572.8 & & \\ & 675.7 & \\ & & 118.8 \end{bmatrix}, \boldsymbol{S} = \begin{bmatrix} 17845 & \\ & 18240 \end{bmatrix}, \boldsymbol{D} = \begin{bmatrix} 1039500 & & \\ & 693000 & \\ & & 68250 \end{bmatrix} \tag{5.3.1}$$

Where $\boldsymbol{K}$ is the flexural stiffness matrix in kN.m^2/m, $\boldsymbol{S}$ is the shear stiffness matrix in kN/m, and $\boldsymbol{D}$ is the axial stiffness matrix in kN/m.

Following the reasoning presented in Section 5.2, the Young Modulus for the floor element is defined as:

$$E_{floor} = \frac{K_x}{I} = 9148\ MPa \tag{5.3.2}$$

For both materials, the Poisson ratio ν is defined as 0.

Vertical deflection

The maximum deflection of the plates (in mm) has been estimated for the set of plates, both orthotropic and isotropic. It must be noted that, in the case of an isotropic material, the FEM software Robot does not compute the deflection due to shear; this is, nevertheless, the case with the orthotropic plate, since it is defined by its stiffness matrix.

Thus, the shear correction is added to the isotropic model, with the formula:

$$\delta_s = \frac{q \cdot w^2}{8 \cdot S_x} = 0.56\ mm \tag{5.3.3}$$

Where S_x is the shear stiffness of the orthotropic material in its main direction. This correction is constant for all the iterations and corresponds to the value at mid-span.

The difference between the orthotropic and isotropic models, expressed as the ratio $\Delta = \frac{|\delta_{ortho} - \delta_{iso,tot}|}{\delta_{iso,tot}}$, is shown in the Figure 5.3.2 below (detailed results are available in the Appendix A.1):

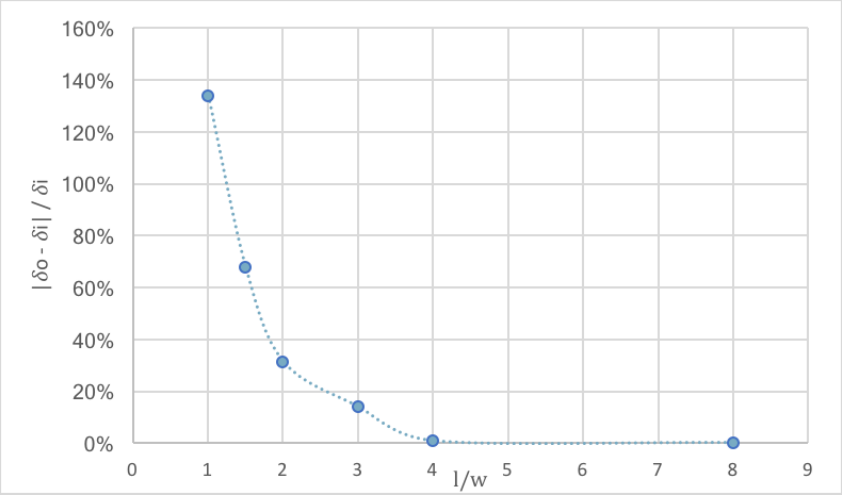

Figure 5.3.2: Evolution of the difference between orthotropic and isotropic model with the l/w ratio

As can be seen from the results, the difference between both model decreases as the l/w ratio increases. The deflection is high from the beginning for the orthotropic plate, and does not vary much with the ratio. This is due to a relatively low stiffness in the length direction ($\frac{K_x}{K_y} \approx 4$), which increases it when both deflections interact, i.e. $l/w \leq 2$. After this threshold, the deflection is stable, confirming the action as a one-way slab.

However, the isotropic plate has the same bending stiffness in both directions; the fact that it is pinned at all of its edges allows the deflection to be minimised, and the two-way slab behaviour is emphasised. Eventually, this becomes negligible after a certain threshold, and the isotropic solution converges towards the orthotropic one. Another notable point is that the deflection induced by shear cannot be ignored, and must be added in the isotropic case to get sensible values.

It is also interesting to compare the limit value to that one would obtain with a hand calculation, assuming a CLT beam:

$$\delta = \frac{5 \cdot q \cdot w^4}{384 \cdot K_x} + \frac{q \cdot w^2}{8 \cdot S_x} \approx 7\ mm \tag{5.3.4}$$

The one-way span assumption for a high length-to-width ratio yields satisfactory results.

Bending moments and transverse shear forces

The evolution of the ratio $\Delta = \frac{|M_{ortho} - M_{iso,tot}|}{M_{iso}}$, along the length-to-width ratio of the orthotropic and isotropic plates, is plotted in the Figure 5.3.3:

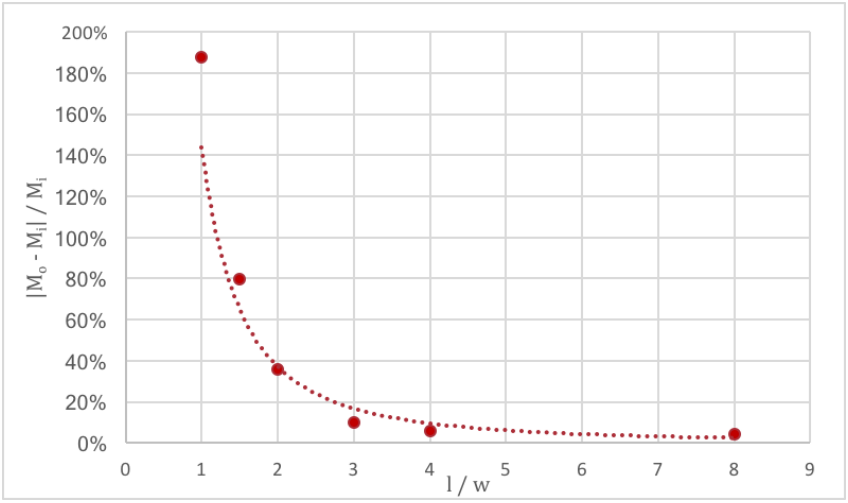

Figure 5.3.3: Bending moment discrepancies between models

Once again, the bending moments follow the same tendency. The bending moments in the orthotropic plate are higher at low l/w ratios due to the interaction of a sensibly lower bending stiffness in the perpendicular direction; but eventually, both converge towards the same value of 10 kNm/m. This phenomenon occurs more quickly in the orthotropic plate.

The most critical discrepancy occurs for a ratio of 1, as shown below:

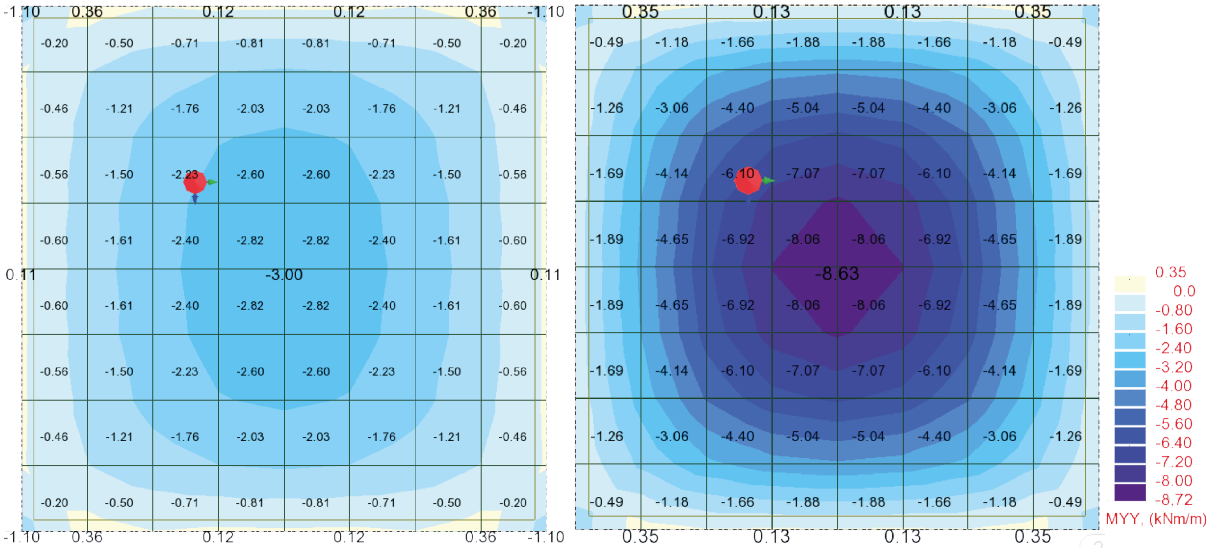

Figure 5.3.4: Bending moment maps for isotropic (left) and orthotropic (right) plates, for a l/w ratio of 1

For such a geometry, the difference in moments in the orthotropic slab are up to 188%.

A check by hand calculation, for a beam under uniform loading, yields the following result, at mid-span:

$$M = \frac{q \cdot w^2}{8} = 10\ kNm/m \tag{5.3.5}$$

Which confirms the assumption of one-way slab behaviour.

The same observation can be made for the shear forces at the supports: the more square a slab is, the more shear it will be subjected to. The comparison between orthotropic and isotropic behaviour is shown for the worst case ($l/w = 1$):

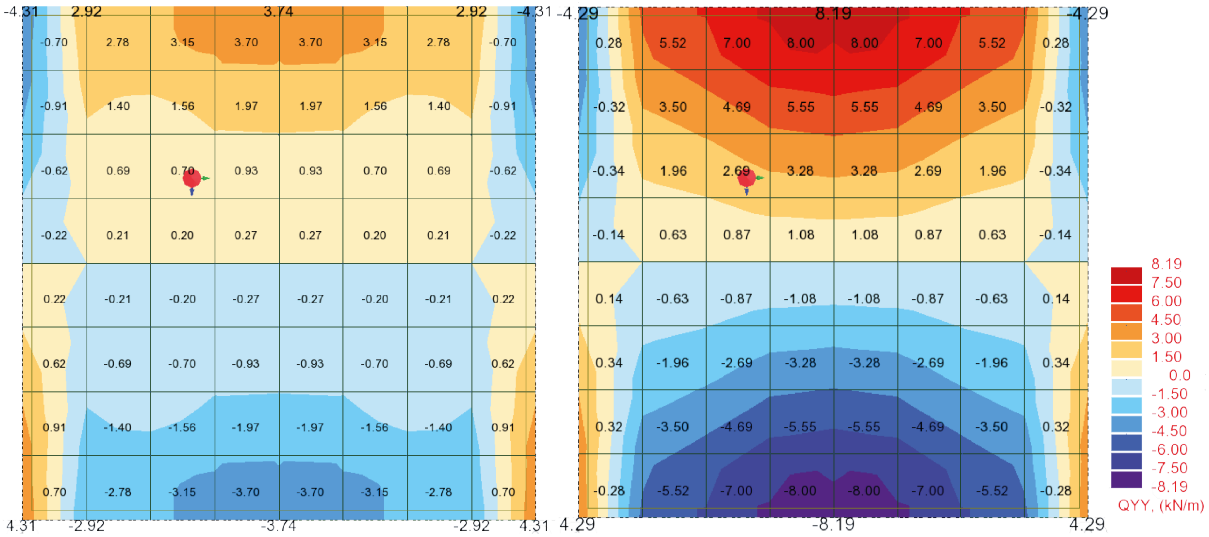

Figure 5.3.5: Shear force maps for isotropic (left) and orthotropic (right) plates, for a l/w ratio of 1

The maps show a difference of up to 120%. Eventually, both values are converging when the slab elongates:

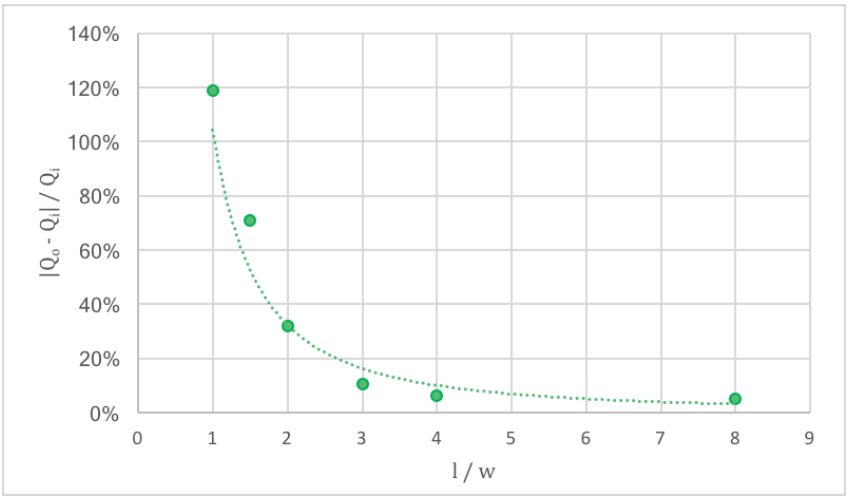

Figure 5.3.6: Shear forces discrepancies between models

By hand, one would get a maximum shear force of:

$$Q = \frac{q \cdot L}{2} = 10\ kN/m \tag{5.3.6}$$

Conclusions on the model validity for floor design

The results teach us that the one-way slab behaviour occurs way more quickly in the orthotropic model, representing the CLT floors more accurately, than in the isotropic one. The influence of a lower bending stiffness in the perpendicular direction implies that the efforts and the displacement will be higher earlier in a real CLT panel, even within a supposedly one-way slab action.

It can be noted that the discrepancy between the two models follow the same trend:

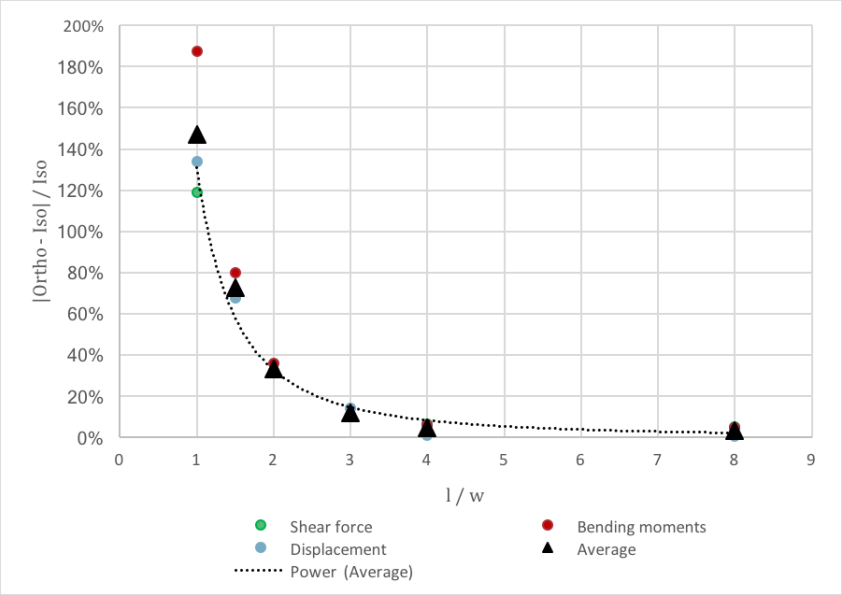

Figure 5.3.7: Influence of the length to width ratio on displacement and efforts values; difference between ortho and isotropic models

On this basis, one could propose to increase the results obtained from the isotropic model, depending on the considered slab dimensions. Nonetheless, more experimentation is needed to ensure that this solution is viable.

In the meantime, the proposed solution is to automatically consider the CLT slab as one-way — spanning along its shorter dimension — and create a sub-model in the Grasshopper framework. The sub-model is entirely independent from the rest of the building, and allows the individual design for slabs under out-of-plane loads. The latter will be considered simply supported along their length, yielding conservative results. Moreover, the deflection caused by shear (Equation 5.3.6) will be added.

5.3.2 Vertical load distribution

In order to perform a global analysis, one has to make sure that the load repartition between elements is accurate with an isotropic modelling of CLT elements. The results will be compared with an orthotropic model for vertical loads.

To check that the global forces acting on a wall are consistent with an isotropic modelling, the vertical load distribution from a slab between 4 walls is studied.

For an isotropic material, the load distribution between walls follows approximately this principle:

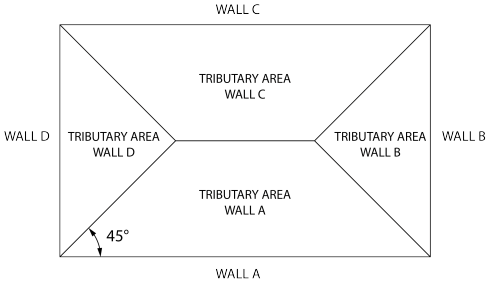

Figure 5.3.8: Vertical load distribution between four walls, following the tributary area principle

The more the length-to-width ratio increases, the more percentage of load will be distributed to the walls along the slab length; the slab behaviour can be approximated as one-way, as explained previously. However, as the conclusion from Section 5.3.1 shows, the one-way slab behaviour takes over much more quickly with the orthotropic CLT panels. The load distribution is therefore likely to be impacted, especially for slabs with a low l/w ratio.

The worst case scenario is considered by evaluating the load distribution from a slab with a l/w ratio of 1 (i.e. square). The percentage of loading that each wall receives is evaluated on the basis of the sum of their base support reactions.

For an isotropic square slab, each wall will naturally get 25% of the load, since the bending stiffness is the same in both directions. This is not the case for a CLT slab: since its bending stiffness is higher in one direction, the walls in the main spanning direction will receive more load, even with a square slab.

It is therefore proposed to carry out experiments with several CLT cross sections, with a varying bending stiffness ratio in cross directions $\frac{K_y}{K_x}$, and compare the percentage of loading to the isotropic distribution (25%) for the most heavily loaded wall.

To this end, a test building was modelled in Robot. The 5x5m slab is supported by 4 walls (cross section as in section 5.3.1), of a 3m height, and is uniformly loaded with 5 kN/m^2.

7 CLT cross sections are evaluated for the slab: the 3, 5 and 7 layers cross sections from Appendix B.1, as well as 4 products from the Stora Enso catalogue [20] [35]; they have been chosen according to their bending stiffness ratios.

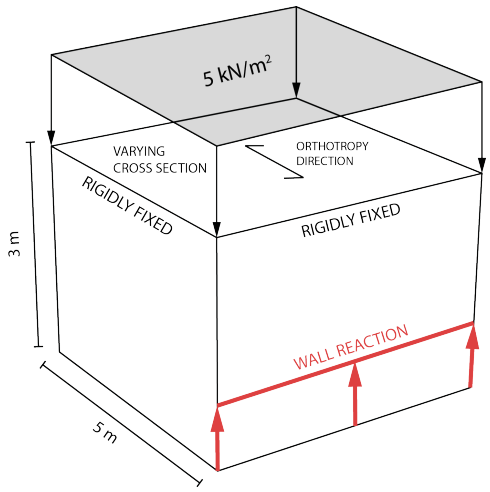

Figure 5.3.9: Simulation setup for the estimation of vertical load distribution in orthotropic slabs

The figure below presents the difference between the loads shared on this specific wall by an isotropic slab and an orthotropic slab, expressed as the ratio $\frac{\%_{Ortho}}{\%_{Iso}} = \frac{\%_{Ortho}}{0.25}$, depending on the ratio between the bending stiffness in both directions:

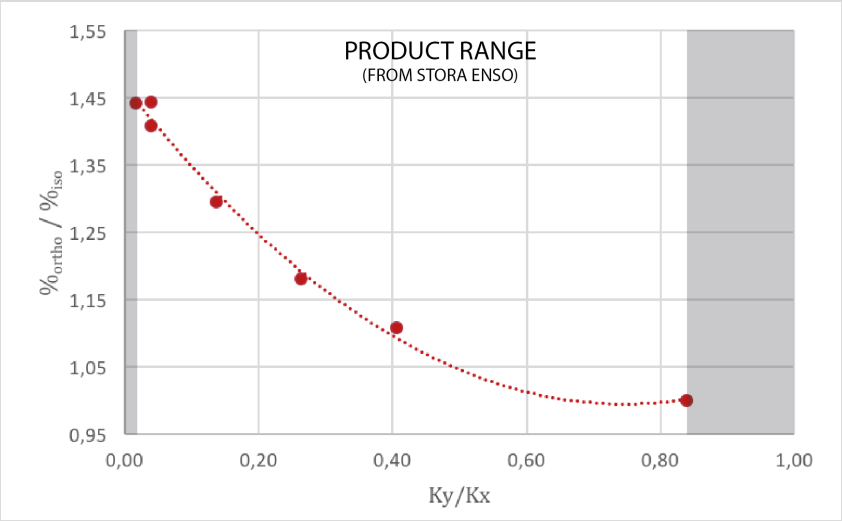

Figure 5.3.10: Variation of the load distribution depending on the cross bending stiffness ratio

In theory, this ratio is not limited, but it is proposed to confer to the product range proposed by Stora Enso [35].

What can be remembered of this study is that the lower the ratio between the two bending stiffnesses, the more the CLT slab will behave as an isotropic one. On the other hand, for CLT cross sections with a higher ratio, the orthotropic model will attract up to 1.5 times the load compared with the isotropic model. This difference is expected to decrease as the length-to-width ratio increases, but cannot be ignored in other cases.

To take this phenomenon into account, it is proposed to define "load bearing" and "non load bearing" walls in the framework, when checking the overall design of a wall for vertical loads.

For a wall defined as load bearing, a safety factor of 1.5 is applied. This would give conservative results for some cases, yet ensure a safe design for walls supporting slabs with a low l/w ratio slab.

5.4 Force distribution in wall elements

The most correct modelling of CLT elements is, as explained above, with the definition of its stiffness matrix. The approach here contemplated uses an isotropic approximation; therefore, the force distribution on an wall, loaded in its plane, is likely to be different between the two models.

To evaluate the impact on the method's results, a simple wall is modelled in Robot Structural Analysis, with the dimensions l x h = 5 x 3 m.

The way loads are carried through the wall element are investigated with both an isotropic modelling and an orthotropic one. The isotropic modelling is based on the 150mm CLT cross section defined previously (E_i = 6930 MPa, ν = 0).

Two types of loads are applied: a uniform vertical load of 5 kN/m, acting on a part of its upper edge (representing the vertical forces); and a uniform shear load of 10 kN/m, distributed along its entire upper edge (representing the wind action). The reason for applying the vertical load on only part of the wall is due to the fact that since both orthotropic and isotropic modelling have a Poisson ratio equal to zero, a uniform load will not give interesting results if applied on the whole wall; on the other end, it is possible to consider the path of such a force if only part of the wall is stressed.

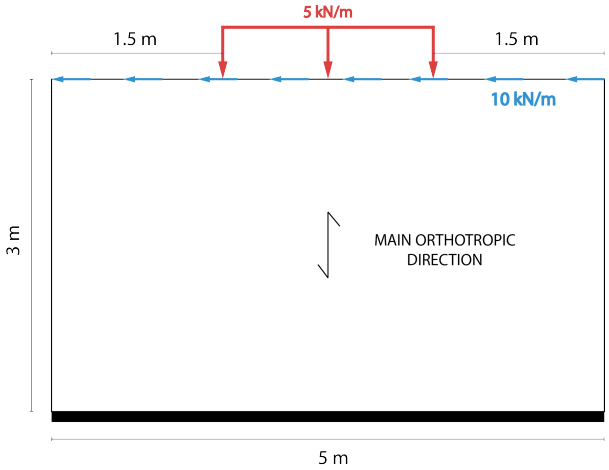

Figure 5.4.1: Simulation setup for the comparison of force distribution in a wall

The possible discrepancies between orthotropic and isotropic models is likely to be linked to the lack of similarity between their in-plane stiffness matrices: while the isotropic material has a an equal axial stiffness in both direction and a relatively high shear stiffness ($G_i = E_i/2$), the orthotropic model will have these two values differ largely, especially regarding the latter. Two sets of tests are therefore performed: in the first one, the orthotropic in-plane stiffness matrix is set to correspond to the isotropic one, to the exception of its axial stiffness in the horizontal direction, which is varied with different $\frac{D_{y,o}}{D_{y,i}}$ ratios. The second battery of tests adopts the same idea, with a varying $\frac{D_{xy,o}}{D_{xy,i}}$.

The amplitude and distribution of each individual force is studied for both cases and loads in terms of vertical and shear forces, to estimate the variations between the reference orthotropic model and the isotropic approach.

5.4.1 First simulation: variation of the axial stiffness

The first test studies the influence of the ratio between the axial stiffness in both direction. The axial stiffness in the main direction is set equal to the isotropic representation, as well as the shear stiffness. The axial stiffness in the horizontal direction is set to vary, with a ratio $D_{y,o}/D_{x,o}$ from 0.8 to 0.1:

$$\boldsymbol{D_{o,1}} = \begin{bmatrix} D_{x,i} & & \\ & D_{y,o} & \\ & & D_{xy,i} \end{bmatrix} \tag{5.4.1}$$

With $D_{x,i} = E_i \cdot t = 1039500\ kN/m$, and $D_{xy,i} = G_i \cdot t = 519750\ kN/m$.

Force distribution from the vertical load

When progressively decreasing the stiffness ratio, the vertical and shear forces in the wall element are modified along the following pattern:

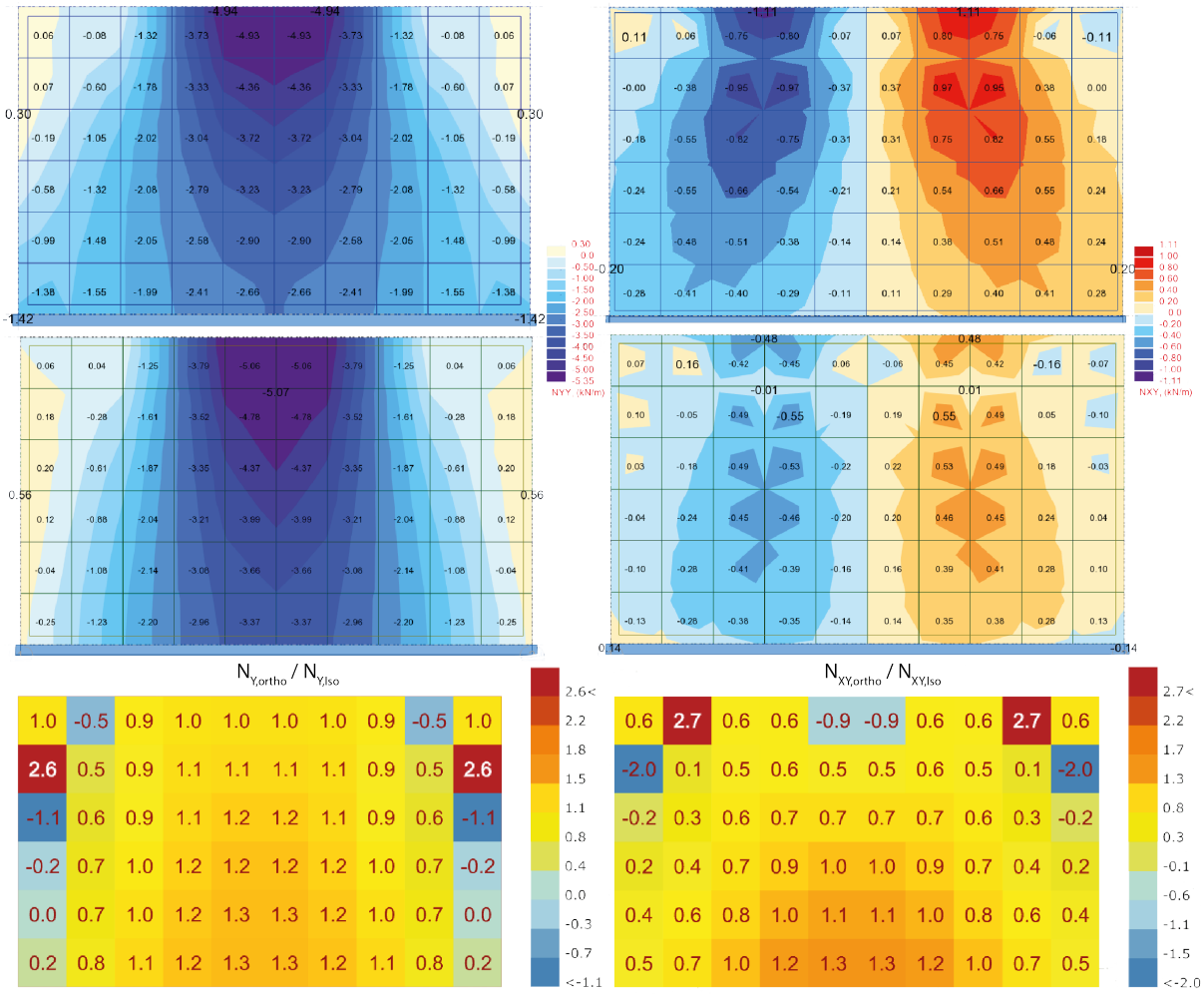

Figure 5.4.2: Comparison of vertical (left) and shear (right) membrane forces in an isotropic (top) and orthotropic material with D_y / D_x = 0.1 (middle). Ratios between orthotropic and isotropic values are shown at the bottom.

The orthotropic maps provided in figure 5.4.2 show the more drastic variation between all the measured values (other maps are available in the Appendix A.3). As can be observed from the top of the figure 5.4.2, the more the ratio D_y/D_x decreases, the more the vertical load is flowing directly to the supports. Indeed, since the horizontal stiffness is relatively lower, less displacement (and therefore force) is created in the horizontal direction. Thus, the portion of the wall directly underneath it is more stressed in an orthotropic material, while it is the opposite at the corners, where the force decreases to 20% of its isotropic counterpart. A significant increase can be seen (260%) on the relative values map, near the top corners. However, its magnitude is negligible compared to other parts of the panel.

On the other hand, to react to a lower horizontal force, a lower shear force results at the load variation points. Once again, the regions at the bottom of the panel experience higher shear forces. However, comparatively to the governing shear force occurring at the top of the isotropic wall (1.11 kN/m),

the forces are always lower in the orthotropic panel; no special measure is needed to counteract the discrepancy between both modellings.

This is not the case for the vertical forces: the vertical force in the orthotropic panel is higher, at its top, than its isotropic counterpart. The Figure 5.4.3 shows the increase of the $\frac{N_o}{N_i}$ ratio for the governing force against the axial stiffness ratio (detailed values available in Appendix A.3):

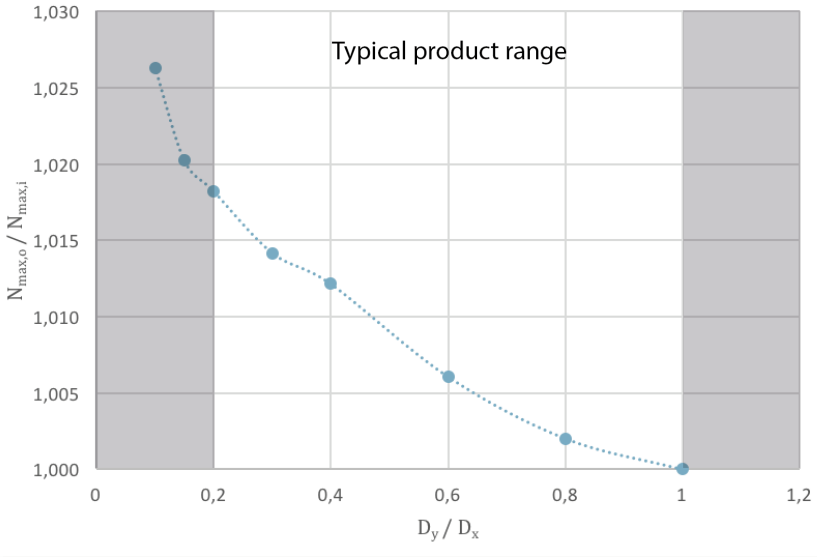

Figure 5.4.3: Increase of the maximum vertical force ratio in the wall against the ratio D_y / D_x

At worst, within the product range offered by the company Stora Enso [35], the maximum vertical stress occurring at the top of the loaded wall is increased by $\approx$ 2%. This percentage is deemed negligible: it is therefore assumed that the variation of the axial stiffness does not have an influence on the governing axial force in compression.

Force distribution from the horizontal load

Equally, the distribution from the horizontal load is analysed:

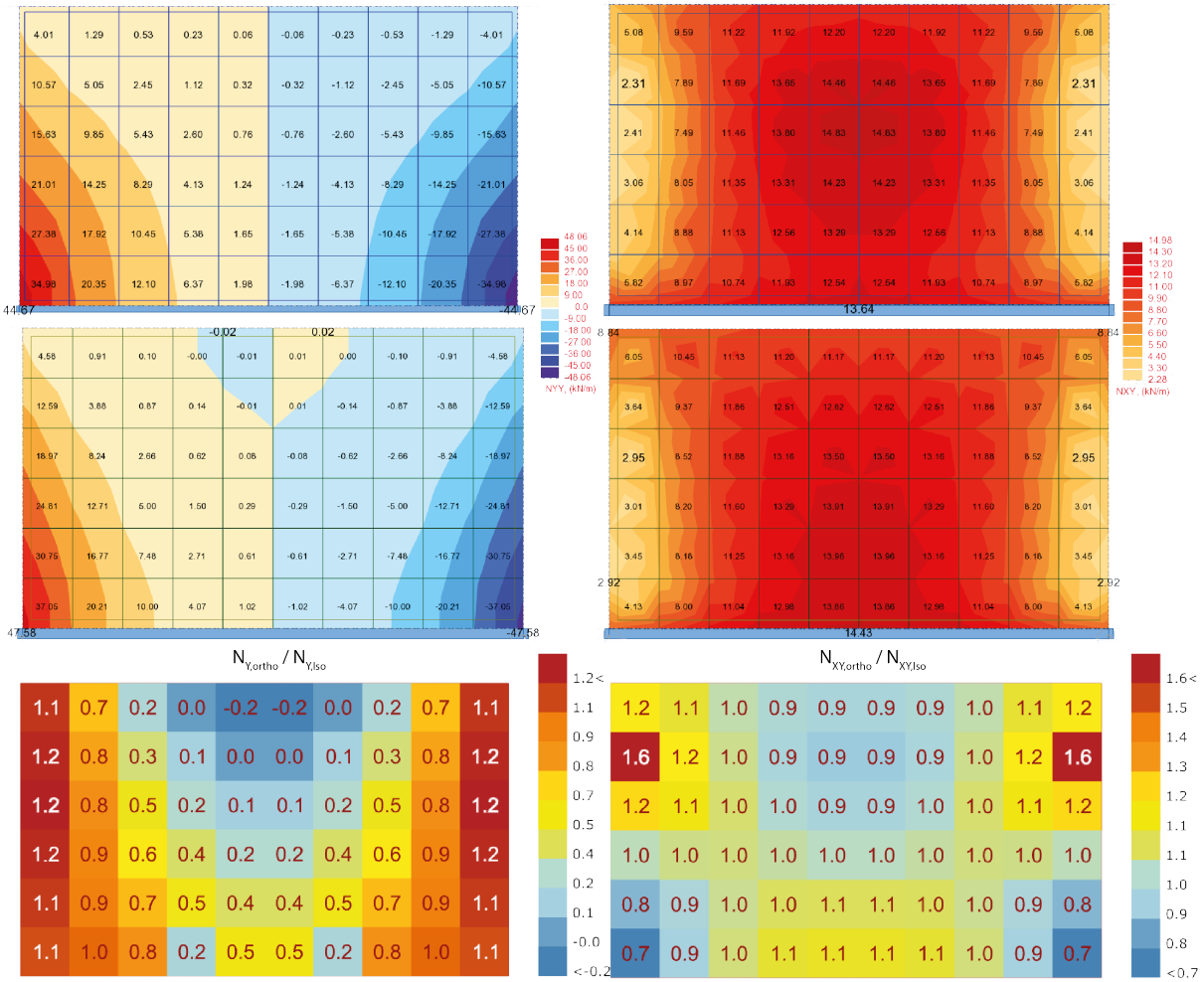

Figure 5.4.4: Comparison of vertical (left) and shear (right) membrane forces in an isotropic (top) and orthotropic material with D_y / D_x = 0.1 (middle). Ratios between orthotropic and isotropic values are shown at the bottom.

As far as the vertical forces in the wall are concerned, the horizontal loading creates tension and compression respectively at each corner. Decreasing the axial stiffness ratio shows, in the worst case, a 20% increase in the vertical edges of the panel. These values are, nonetheless, always lower than the maximum force acting at the bottom corners, and are thus not governing the design. The latter shows a slight increase compared to the isotropic material; within the Stora Enso product range [35], it tops up at ≈ 2%, as shown by the Figure 5.4.5 (tabulated values in Appendix A.3):

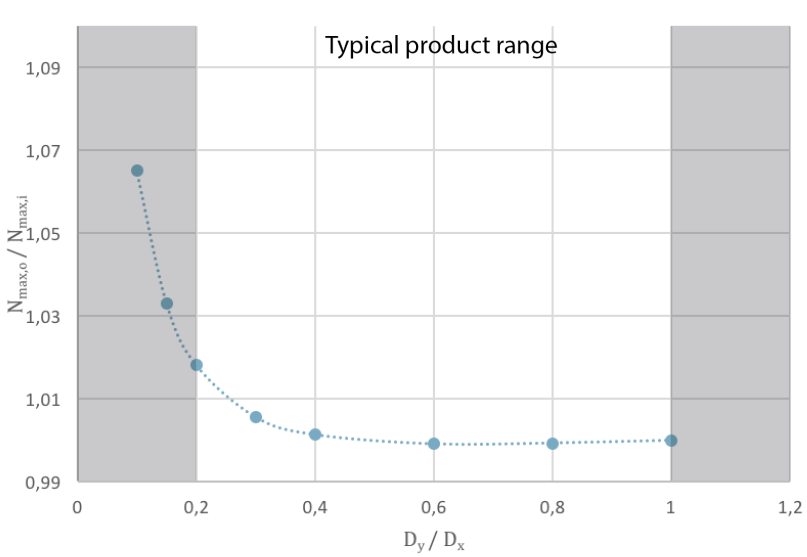

Figure 5.4.5: Increase of the maximum vertical force ratio from a shear loading against the ratio D_y/D_x

This increase is minimal and will not be taken into account for the model calibration. Moreover, the normal force in the central part of the wall is decreased.

Regarding the shear forces, their distribution slightly varies between the orthotropic and isotropic models. The maximum shear force occurs at the bottom of the orthotropic wall (centre in the isotropic model), and is higher at the vertical edges and top corners. However, it is never higher than the governing isotropic force.

Intermediate conclusion

As seen for this set of simulations, the variation of the horizontal stiffness does not have a significant influence on the maximum forces; the results obtained by the isotropic model will be considered accurate regardless of the cross axial stiffness ratio.

5.4.2 Second simulation: variation of the in-plane shear stiffness

The same procedure is carried on for a second battery of simulations, this time varying the ratio between the orthotropic and isotropic shear stiffness. Both axial stiffness values of the orthotropic model are set to the isotropic ones.

$$\boldsymbol{D_{O,2}} = \begin{bmatrix} D_{x,i} & & \\ & D_{y,i} & \\ & & D_{xy,o} \end{bmatrix} \tag{5.4.2}$$

This time, the ratio $D_{xy,o}/D_{xy,i}$ is varying. This ratio can also be expressed in this way:

$$\frac{D_{xy,o}}{D_{xy,i}} = \frac{2 \cdot G^* \cdot t}{E_{0,CLT,mean} \cdot t_0} \tag{5.4.3}$$

Using equation 3.3.6, it is possible to determine the minimum value of this ratio by assuming a non edge-bonded CLT layup ($G_{CLT,mean}$ = 450 MPa) with $t = t_0$, and the limitation on the layer thickness and board width from the EN 13651 [11], respectively $t_l \geq 6$ mm and $w_l \leq 300$ mm; the minimum ratio of 0.02 is obtained and is used as the lower boundary for the study. The same reasoning leads to an upper boundary (≈ 0.22).

Force distribution from the vertical load

The highest variation between the results, obtained for a ratio $D_{xy,o}/D_{xy,i} = 0.02$, is shown below for the vertical load case:

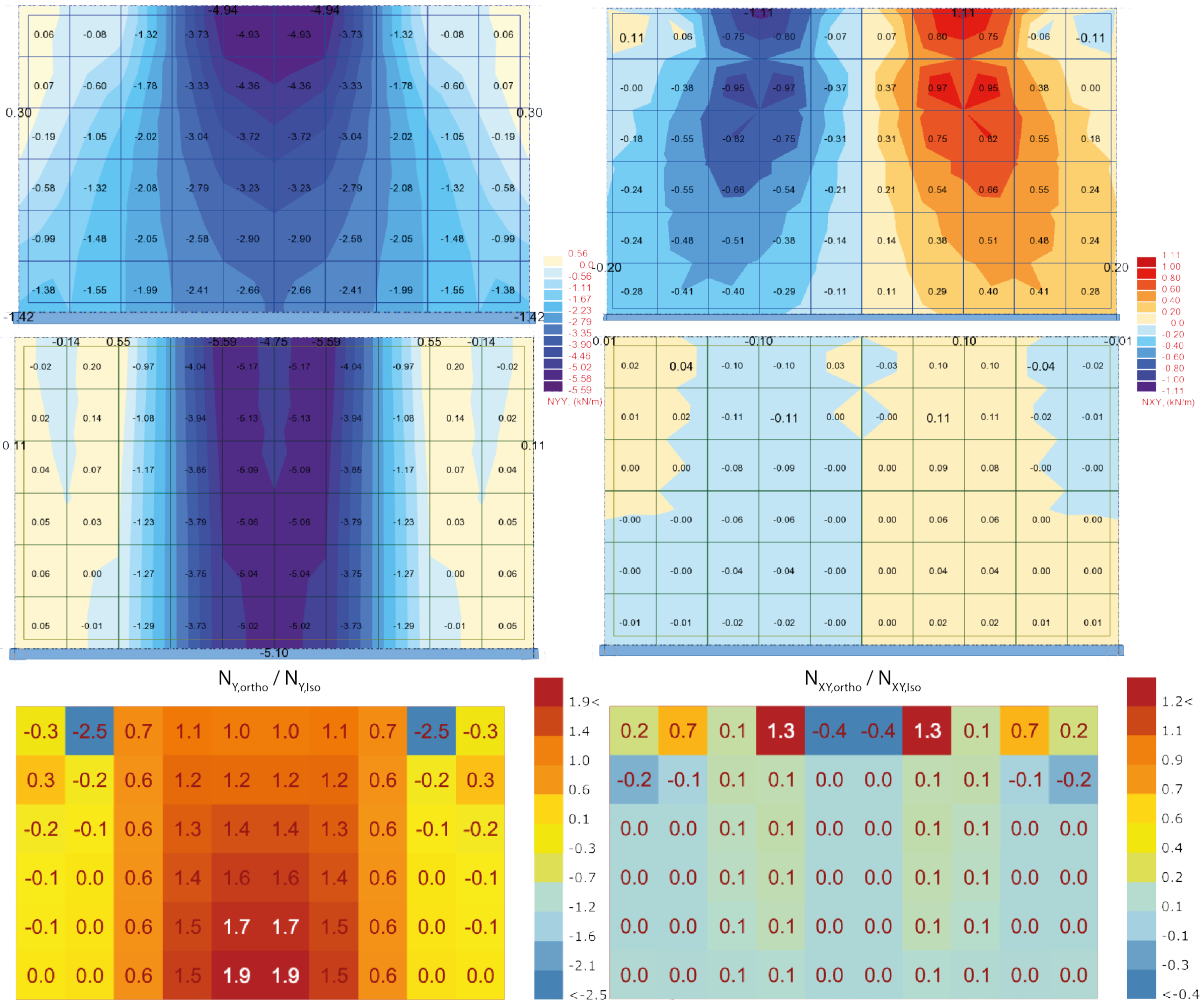

Figure 5.4.6: Comparison of vertical (left) and shear (right) membrane forces from the vertical loading, in an isotropic (top) and orthotropic material with $D_{xy,o}$ / $D_{xy,i}$ = 0.02 (middle) Ratios between orthotropic and isotropic values are shown at the bottom.

Similarly as with the first simulations, when the shear stiffness ratio decreases, the vertical load flows right down to the wall supports. Since the vertical axial stiffness is much higher, almost no shear force occurs in the panel, resulting in an almost pure vertical stress. The area just below the load will therefore endure higher forces, since almost none are dissipated through shear and horizontal load. While not governing the design, the rise goes up to almost twice the isotropic values. The shear

force decreases with the shear stiffness ratio, up to a point where it is quasi nonexistent. The highest increase at the top is indeed insignificant in amplitude compared to the isotropic values.

The only potential issue with an isotropic modelling is thus the governing vertical force in the orthotropic panel, which is higher than the corresponding isotropic force. It follows the trend below:

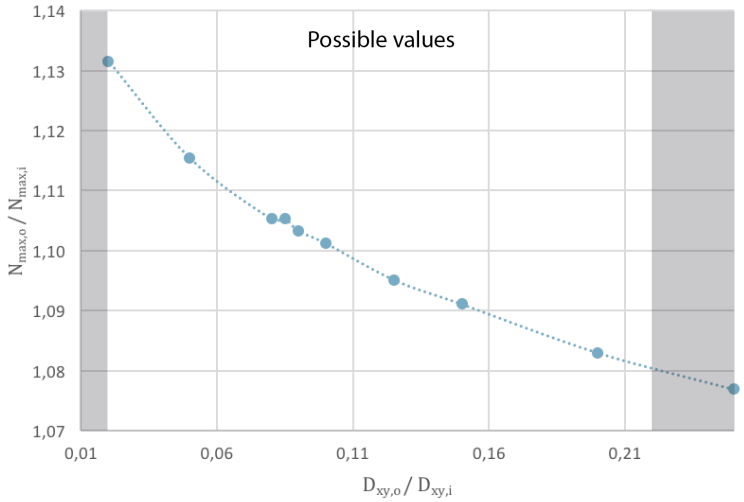

Figure 5.4.7: Increase of the maximum vertical force ratio from a shear loading against the ratio $D_{xy,o}$ / $D_{xy,i}$

The decreasing shear stiffness ratio has a higher impact on the maximum vertical force than the axial stiffness ratio: up to $\approx$ 13% more load is to be found in the panel. The values are not too scattered and vary between 8 and 13%; proposing an increase based on the latest value, regardless of the actual ratio, does not seem disproportionate and will be discussed.

Force distribution from the horizontal load

Finally, the effect of a horizontal loading is simulated, yielding the following results for the vertical and shear forces:

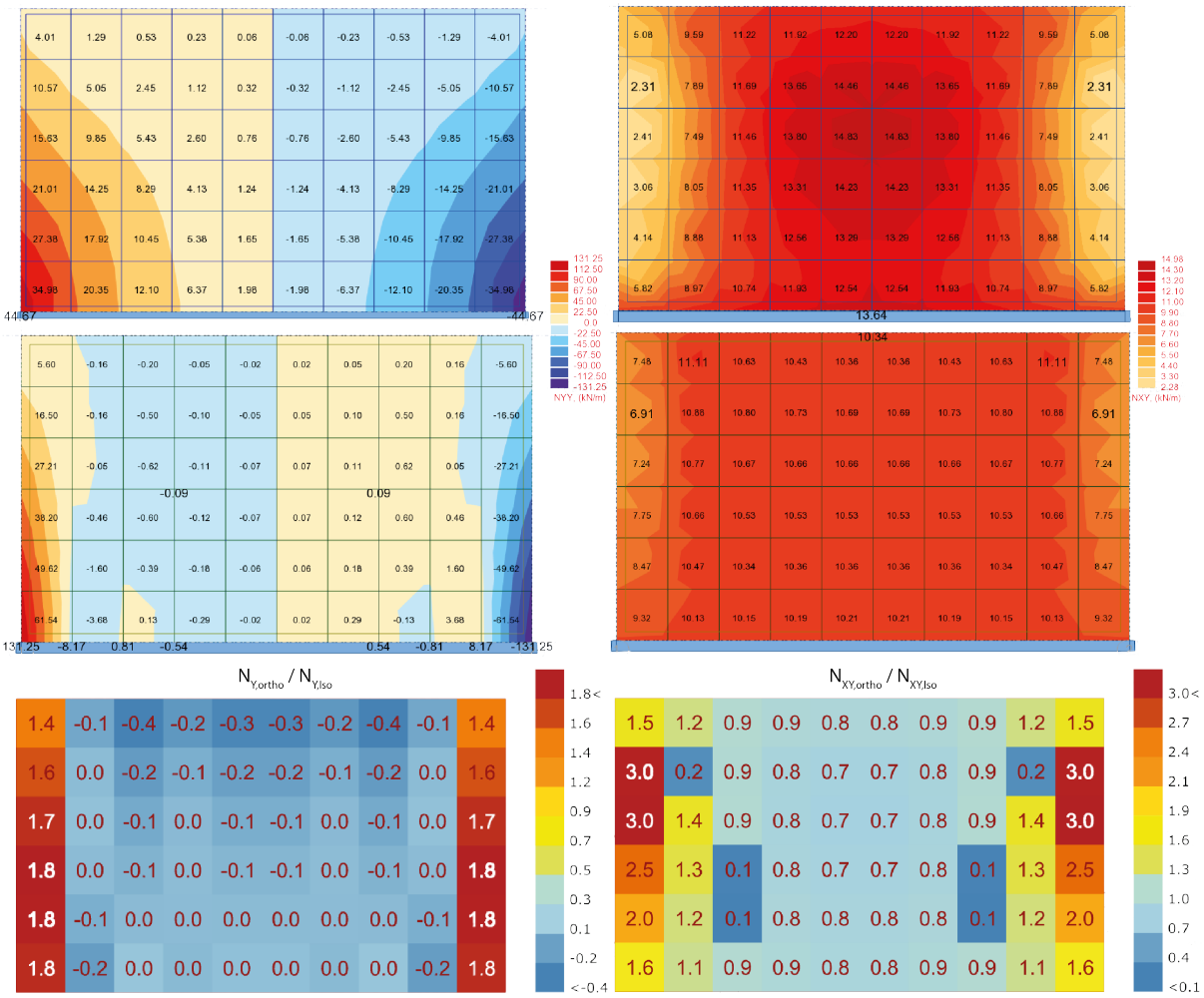

Figure 5.4.8: Comparison of vertical (left) and shear (right) membrane forces from the shear loading, in an isotropic (top) and orthotropic material with $D_{xy,o}$ / $D_{xy,i}$ = 0.02 (middle). Ratios between orthotropic and isotropic values are shown at the bottom.

As the shear stiffness ratio decreases, the shear load spreads less in the wall area: the shear force decreases and becomes almost uniform, to the exception of the vertical edges. In any case, the critical shear force in the orthotropic model is always lower than in the isotropic one (more force maps in Appendix A.3). However, the ratio has a critical importance on the tension and compression that is created. The more it decreases, the more the vertical loads are concentrated at the corners and vertical edges (up to 1.8 times the force experienced in the isotropic panel), while the remainder of the panel is left almost unstressed. This leads to very high loads: for a shear stiffness ratio of 0.02, the resulting load at the corner is almost three times higher in the orthotropic model than it is in the isotropic material:

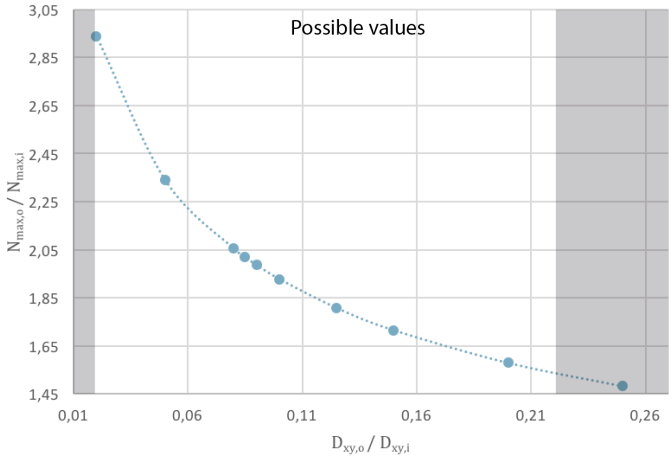

Figure 5.4.9: Increase of the maximum vertical force ratio from a shear loading against the ratio $D_{xy,o}$ / $D_{xy,i}$

Such influence cannot be ignored, if a safe design is to be undertaken. However, the values related here are applied for a 3m high wall, and might not be true in the general case; indeed, while increasing the height of the wall, it has been noted that the discrepancy between orthotropic and isotropic values decreased. To keep on with this characterisation, it is proposed to realise a few more simulations with different wall heights, this time considering the combined in-plane stiffness of the wall:

$$D = \frac{3 \cdot D_x \cdot D_{xy}}{3 \cdot D_x \ H + D_{xy} \cdot H^3} \tag{5.4.4}$$

The same simulation was carried out with the same parameters, but this time with a varying wall height, at 6, 10 and 25 meters. The results were plotted against the ratio of the combined stiffness of the orthotropic panel over the isotropic panel, $\frac{D_{ortho}}{D_{iso}}$:

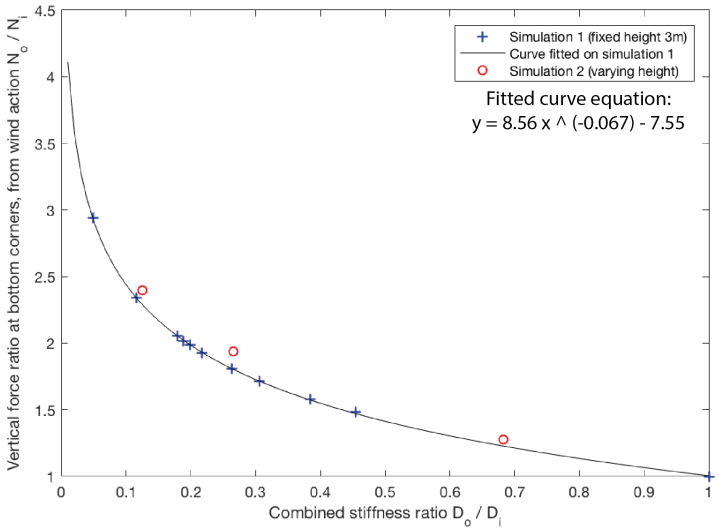

Figure 5.4.10: Increase of the maximum vertical force ratio from a horizontal loading against the combined stiffness ratio D_{ortho} / D_{iso}

Detailed values are available in the Appendix A.3.

The curve fits perfectly the first set of simulations; moreover, the three test values, even though small in number, seem to follow this tendency with relatively little difference: in average, the values that are obtained are less that 5% higher that the predicted ones. This prediction of the vertical force increase in the orthotropic material is deemed accurate and can be used in the design to calibrate the isotropic model.

5.4.3 Impact on the governing force for walls

From these two sets of simulations, important conclusions can be drawn. With more or less influence, the variation of CLT properties in both direction, as well as a considerably reduced shear stiffness, modifies the force profiles in the wall element. Shear forces, whether they are generated by vertical or horizontal forces, have a tendency to be lower than in the isotropic materials, and in some cases to disappear completely for the benefit of vertical forces (Figure 5.4.7). Due to a reduced shear stiffness, they are more concentrated around the edges of the panels, where they happen to be higher; it is however noticeable that they remain lower than the maximum force happening with the isotropic modelling.

On the other hand, the vertical forces always reach a point where they are critical, whether it happens at the top of the wall (for a vertical load) or at the bottom corners (horizontal load). In this situation, it is interesting to compare the influence of the different parameters that were evaluated:

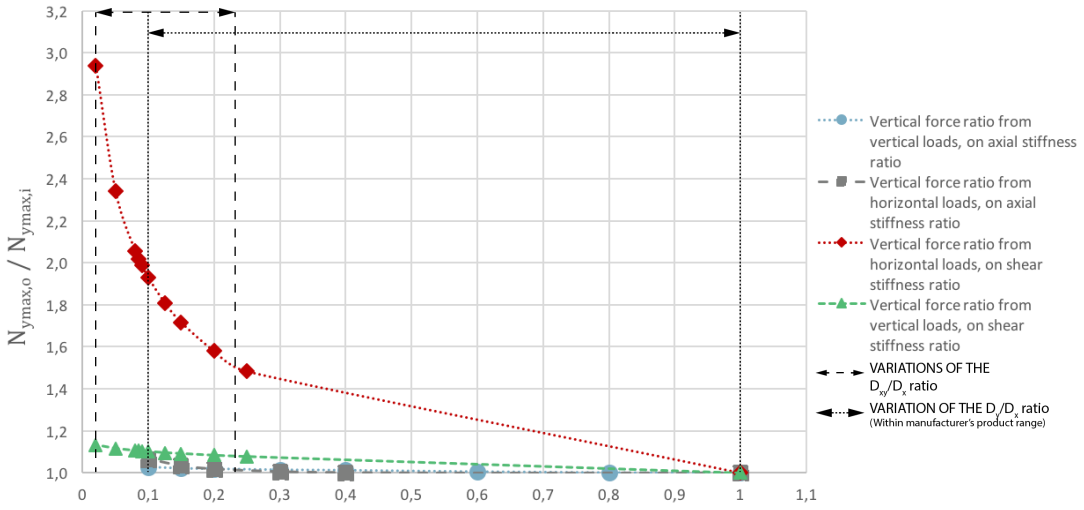

Figure 5.4.11: Comparison of the influence on vertical forces between the several evaluated parameters

Without any doubt, the most influential parameter in both situation is the reduced shear stiffness that defines the CLT material, in comparison with a purely orthotropic material. This impact is more clearly visible on the vertical forces that are created by a horizontal action: they are up to 3 times higher than what can be obtained with isotropy, while the other discrepancies stagnate at a maximum of 1.15. This could cause serious safety issue when performing the structural design of wall elements, and absolutely needs to be compensated.

Based on the Figure 5.4.10, a safety factor γ is proposed, taking into account the combined stiffness ratio of the wall, and calculated with the equation of the fitted curve, in an attempt to increase the stresses in the isotropic walls due to the wind loads:

$$\gamma = 8.56 \cdot \left(\frac{D_{ortho}}{D_{iso}}\right)^{-0.067} - 7.55 \tag{5.4.5}$$

Where D_{ortho}/D_{iso} is the ratio of the orthotropic combined stiffness over the isotropic one of the wall in plane, cf. Equation 5.4.4.

Even so, there is another important aspect which must be accounted for. In general, the vertical load resulting from the slab action will be less concentrated at corners, as shown by the transverse shear force maps on Figure 5.3.6. Besides this, it was observed that in such situation, the compression force at the corner of the wall are higher with an isotropic modelling that with an orthotropic one: up to 5 times for the lower axial stiffness ratio. For the lower shear stiffness ratio, these force is even missing for the section with the lowest shear stiffness ratio (5.4.6).

This has two consequences: on the bright side, the compression resulting from the wind action will be inflated by the existing force at the corners in the isotropic model, granting a conservative design. On the other hand, this will also cause a reduction in the tensile force. To compensate for this, it is suggested to implement a safety measure, aiming at cancelling completely the vertical imposed loads via an optional output to the *Wall Design* component (see Framework Manual, Section 6.3). When activated, a factor of 0 is simply applied to the Imposed Loads applied on floors, relieving wall corners subjected to tension. It is recommended to toggle this option when assessing the design of walls subjected to an overturning moment.

5.5 Proposed corrections to the results

The simulations that were undertaken in this section allowed to cover a significant range of mechanisms that occur in force transfer between the horizontal and vertical structural elements. Starting from the slab design, to the load transfer to and in walls, several parameters were considered to evaluate the difficulties than one can face when considering an hypothetical isotropic material in place of a more correct orthotropic definition of CLT.

As of now, and since no orthotropic material can yet be materialised within the parametric design framework, a few measures must be taken to approach the stress values that can be experienced in a CLT cross section, or at least provide a more conservative design.

Slabs will be emancipated from the rest of the building in order to allow a one-way span calculation, including shear displacements; this is likely the best way to approach the stresses and deflections that develop in a CLT slab, with an isotropic material. This is realised with the *Slab Design* component (see Framework Manual, Section 6.4).

On the other end, walls cannot benefit from such an isolation, and their design solely makes sense within the overall building frame. Two factors are proposed: a 1.5 factor for walls designated as "load bearing", as well as a correction factor for wind based on their combined stiffness ratio. Finally, the potential tension should be evaluated without the contribution from imposed loads. All of these implementations are available within the *Wall Design* component, detailed in the Framework Manual, Section 6.3.

In the end, in order to provide a better control on these factors, the load application has been made in a different way that what was considered initially. While the load combinations were directly used as inputs for Karamba, it is suggested to instead apply only the load characteristic values, and apply the partial factors as a post processing input. In this way, their resulting action on the structure can be individually handled after the analysis.

Chapter 6

Results

In order to assert the applicability of the framework on a real project, its implementation has been tested on a case study, the *Puukuokka* housing block by OOPEAA. This chapter presents this project, and illustrates the feedback provided to the framework's users.

6.1 Case study: Puukuokka Housing Block

Puukuokka is a residential building in Jyväskylä, Finland. It was completed in 2015, and notably won the Finlandia Prize for Architecture as the first eight-storey timber building in Finland. It consists in a complex of three apartment blocks, totalising around 150 flats for a floor surface of 10 000 m^2 [46].

Figure 6.1.1: Puukuokka housing block by OOPEAA

Wood is strong in the expression of Puukuokka, ornamenting its façade but also the interior of the apartments, giving to the living spaces warmth and quality. The structure is made of prefabricated CLT modular elements manufactured by Stora Enso, such as the ones presented in section 2.3. This makes for a robust system, easy to install and flexible over time.

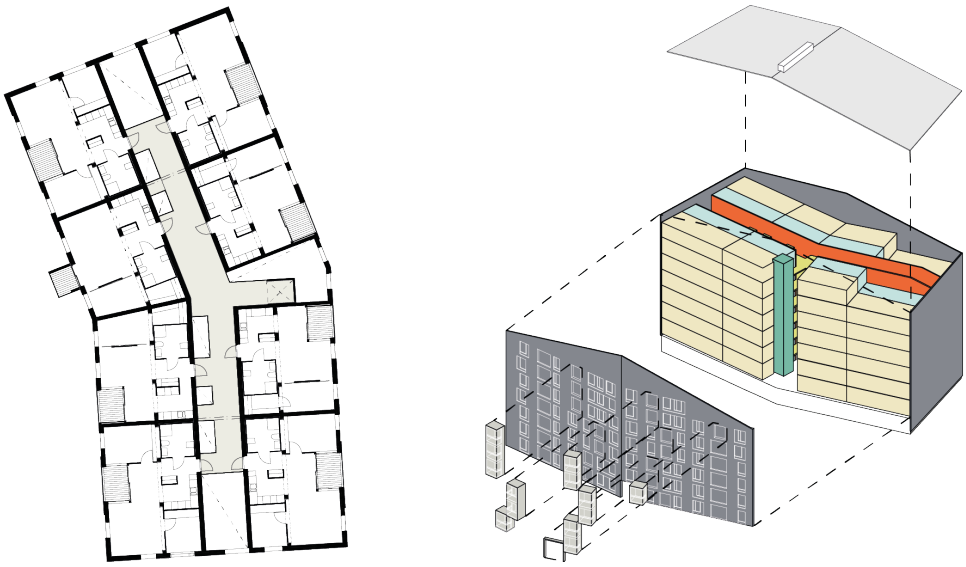

Figure 6.1.2: Apartments layout (left) and modular concept (right)

The concept behind Puukuokka's design is ideal to illustrate the framework, inspired by prefabrication and modular elements, hence this choice. The case study aims at suggesting how such project could be designed with the framework that has been developed.

6.2 Generation of the geometric model

The framework's process has been applied to the Puukuokka project in order to showcase its potential on an existing project. As mentioned above, the housing project consists in an assemblage of modules, that are fairly similar to each other. Thus, it is a perfect example of the genotype/phenotype concept presented in chapter 4, since it consists in a general pattern of designs, adapted in a local context.

The general framework's guide (cf. Framework Manual) has been implemented to generate the building geometry, material and load definition, and structural analysis. The floor plan is used as a basis to define the global layout as illustrated below:

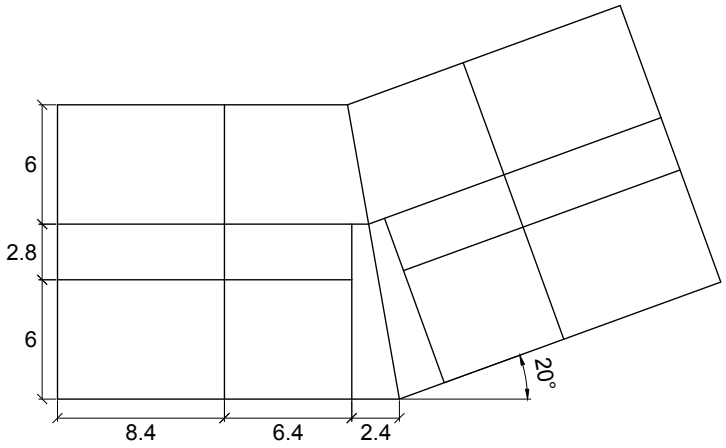

Figure 6.2.1: Floor plan layout used to define the Puukuokka volume

Additional drawings such as sections provided additional information, namely the number of storeys (8), their height (3.4 m), and the roof ridge height (3.2 m).

Using the *Genotyper* component (see Framework Manual, Section 2.1), five Wall Genotypes were created to reflect the project's architectural specificity. They were then used to populate a parametrically defined model, thanks to the *Phenotyper* component (cf. Framework Manual, Section 2.2).

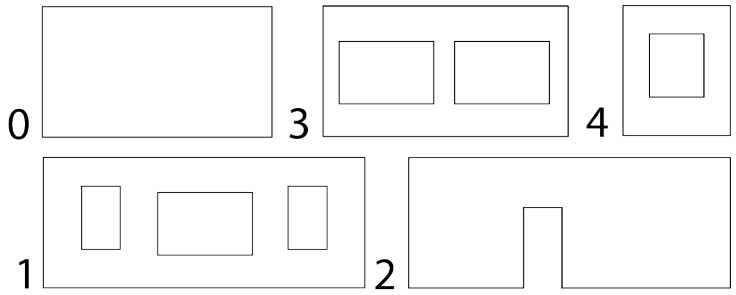

Figure 6.2.2: Wall Genotypes created for the case study building

The Puukuokka housing project would not be complete without its duopitch roof, though. Its design, along with a set of walls and roof elements, was added to the general structure to finalise the digital representation of the structure, as seen in the Figure 6.2.3.

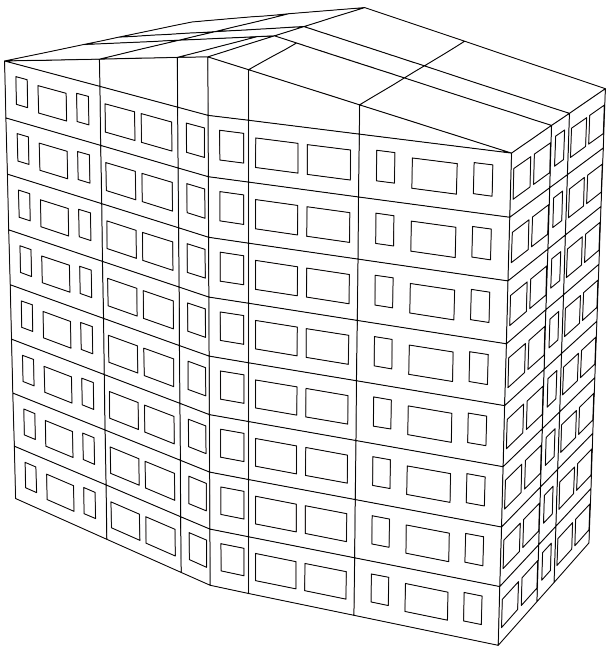

Figure 6.2.3: The Puukuokka model at the end of the population stage

Ensuing the definition of a few CLT cross sections and the load application (cf Framework Manual Sections 3 and 4), the geometric model was analysed and the structural design could begin.

6.3 Design feedback

After the analysis by the Karamba plug-in, all the necessary information is available to evaluate the structure's compliance with safety requirements. The three main outputs will be showcased in this section, namely the horizontal sway, the wall design and slab design. The order in which they are presented is a suggestion to the designers to operate on the results, from the most to the least critical considerations.

6.3.1 Horizontal sway

Since the use of CLT technology continues to grow, the application of this structural system might be seen in larger scale projects such as high-rise buildings. As the storey number increases, the impact of horizontal actions, especially the wind, becomes more and more critical. In this case, the horizontal stability usually governs the design as the maximum sway is limited by the criteria $\delta \leq H/500$ where H is the building's height. This value has to be controlled for Serviceability Limit States load combinations (SLS, cf. Framework Manual Section 4.6).

For that reason, one of the first design tasks should be to ensure that the structure has enough stiffness to respect this criteria. For a shear wall lateral system such as this one, this calls for a reasonable arrangement of internal walls in both direction, and/or, if the façade is to contribute to this resistance, a considerable reduction of its openings. One has to find the right balance between internal flexibility and exterior aesthetics.

To help in this stiffness evaluation, the *Horizontal Sway* component has been developed, and yields the horizontal displacement at the top of the building (for more details and information on its operation, cf. Framework Manual, Section 6.2). An approach on how to use it to solve stability issues will be presented.

Fortunately, the building which is the subject of investigation here does not need to compromise between these. Indeed, as a housing project featuring a repetition of enclosed space, internal flexibility is not a major issue and there are plenty of possible locations for shear walls. Moreover, culminating at 8 stories, the influence of wind is kept at a minimum. For that reason, and to showcase the problem solving workflow, its height has been increased to 71.20 m, accounting for 20 levels.

As a first attempt at evaluating the design, it was assumed that maximal internal flexibility was a desired output. The building was therefore cleared of all its internal walls; such setup as a stabilising system could be assimilated to a framed (beams and columns) structure, for example.

After analysis by the *Horizontal Sway* component, the results were, as expected, unsatisfactory for the characteristic load combination with leading wind load (governing in this case, see Equation 4.19 in the Framework Manual). A look at the output from the component informs on the maximum horizontal displacement:

```
HORIZONTAL DISPLACEMENT
Max. allowed: H / 500 = 142.4 mm
-------------------------------------
Remember: the load cases that should be
checked are the SLS characteristic
combinations
-------------------------------------
If the criteria is not fulfilled:
- Increase wall thickness
- Reduce wall openings
-Add internal shear walls

Load case5 - 319.99 mm  - NOT SATISFIED
```

Figure 6.3.1: *Horizontal Sway* component output for the initial design

Aware that such a design is not really conceivable without additional stabilising system, it was then decided to add internal shear walls in both direction, partly appearing on Figure 6.3.2:

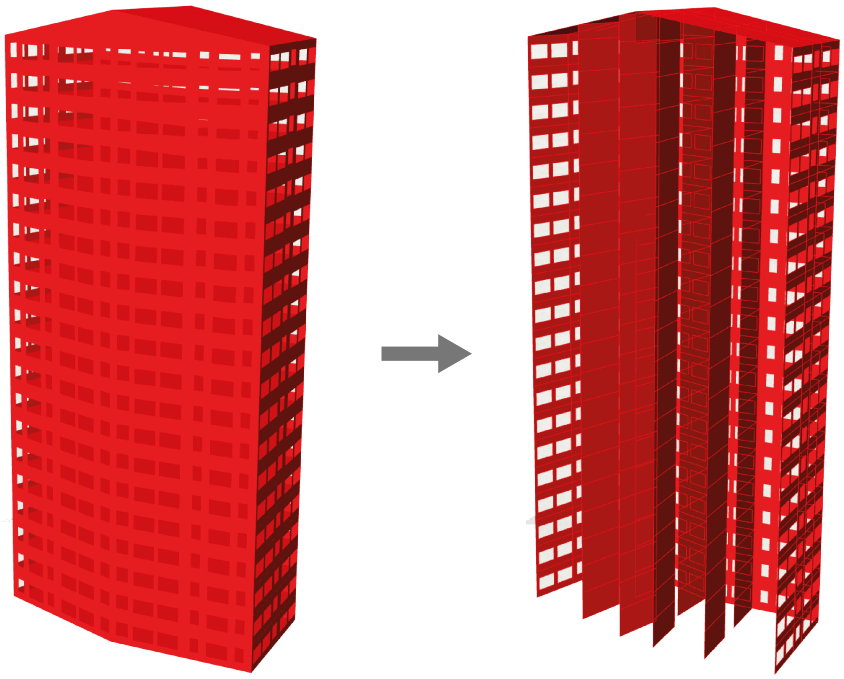

Figure 6.3.2: First structural modification: addition of internal walls

This modification, while greatly reducing the sway, was not enough to satisfy the criteria. A last implementation is needed: this could be increasing the internal walls thickness, which is the least harmful for the building aesthetics. In some cases, this might not be possible: for example, the net area of the building could have been agreed with a customer, or by regulations, making this scenario impossible. To suggest a broader range of action from the designer, it has been chosen to increase the façade stiffness along wind (sides). In other terms, the opening area was greatly reduced. In the method's workflow, this is just a matter of switching the wall types that are attributed to the corresponding Frames.

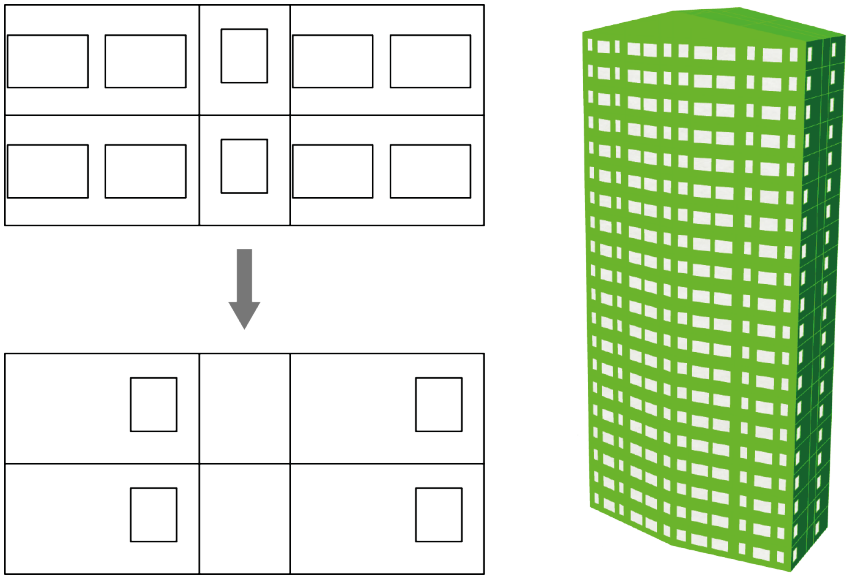

Figure 6.3.3: Modification of the façade design to increase its stiffness and resulting visual feedback

In this way the façade will be able to contribute to the stabilising action. This leads to a positive output from the *Horizontal Sway* component, with a displacement of 112.32 mm $<$ 142.4 mm (maximum allowed).

The structure now fulfils the requirements for horizontal stability. Thanks to the *Horizontal Sway* component, the designer can have a direct feedback on the proposed design efficiency for such criteria. At this stage of development, the component does not reflect the real behaviour of the structure and the deflections are underestimated (this will be discussed in Chapter 7); however, this can be used to evaluate the relative performance of different designs.

6.3.2 Vertical elements design - Walls

The next task that is advised here is to perform the structural design of wall elements, which will carry all the loads, vertical as well as horizontal, to the foundations. Walls are a critical part of the structural safety of a building and should be given the necessary attention. Using the *Wall Design* component, of which the details are addressed in the Framework Manual, Section 6.3, it is possible to get feedback on how a specific wall behaves.

Two types of walls are considered: a solid shear wall without openings, and a façade wall (see Figure 6.3.4) to propose an approach to their respective design. Once again, it must be noted that the Puukuokka design did not present any particular issue regarding structural safety. In an attempt to showcase the framework potential, the vertical and horizontal loads were increased (sometimes up to 4 times) and adjusted to provide a wide range of scenarios.

Figure 6.3.4: Considered walls for the examples

Design of a solid shear wall

Such elements display a high in-plane stiffness, and for good reason: together, they are the main stabilising element for horizontal actions. This also means that they will "attract" most of the horizontal loading, be subjected to high in-plane forces and prone to shear failure.

Given its location and the wind direction, the shear wall used as an example is furthermore solicited in tension, due to a global overturning moment on the building. A first look at the wall support reactions and the textual outputs of the *Wall Design* component confirms this tendency:

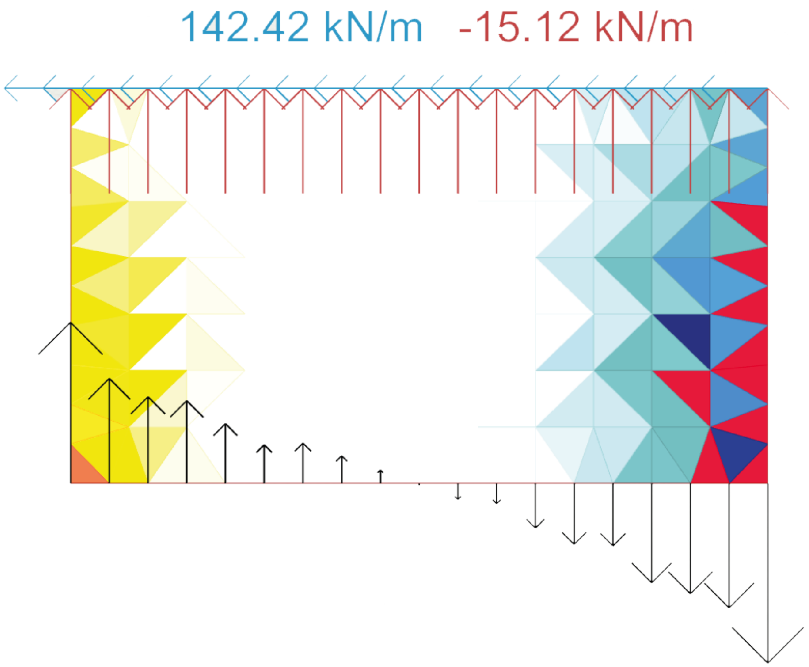


```
COMPRESSION STRENGTH: SATISFIED
----------
Sigma c, max = 15.81 MPa (Load Case 2)
fc,0,d = 18.0 MPa
TENSILE STRENGTH: NOT SATISFIED
----------
Sigma t, max = 17.78 MPa (Load Case 2)
ft,0,d = 11.52 MPa
----------
Tension is too high in the wall. To avoid this:
- Increase the wall effective area (thickness / number of parallel layers)
- Increase the wall grading (CLT24 to 28)
SHEAR STRENGTH: NOT SATISFIED
----------
Tau v, max = 6.02 MPa (Load Case 2)
fv,d = 3.96 MPa
----------
Shear is too high in the wall. To avoid this:
- Increase the average layer thickness (both parallel and crosswise)
TORSIONAL SHEAR STRENGTH: NOT SATISFIED
----------
Tau T, max = 2.41 MPa (Load Case 2)
fT,d = 1.8 MPa
----------
Torsional shear is too high in the wall. To avoid this:
- Increase the average layer thickness (both parallel and crosswise)
- Increase the board width within the normative limits (≤ 300 mm)
```

Figure 6.3.5: Support reactions and global loads shown with the vertical stress force maps; textual outputs (right)

The wall is globally subjected to an uplift force of 15.12 kN/m, as well as a significant shear force (142.42 kN/m). A failure in tension is already visible at the right corner, which is consistent with the forces the wall is taking. The output messages inform the designer that the wall is failing in tension, shear and torsional shear: its design must be improved. The solution to this issue consists in modifying the cross section attributed to the wall. At this stage, the wall is set with a 90 mm cross section, with 3 layers (30-30-30) arranged crosswise.

By looking at the stress maps, it is possible to get a hint on which failure is the most decisive:

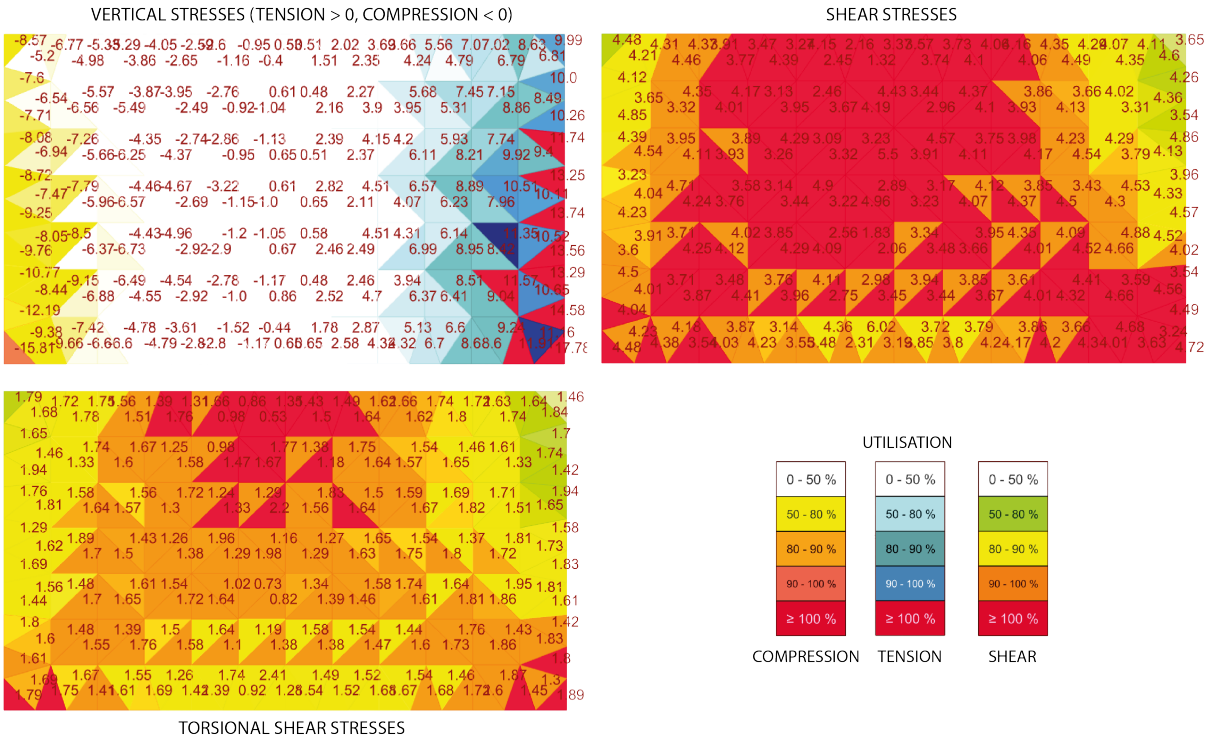

Figure 6.3.6: Stress maps and values - vertical stresses (top left), shear stresses (top right) and torsional shear stresses (bottom)

As can be seen from Figure 6.3.6, the shear failure occurs in almost the entire wall; it is the first issue that will be corrected. Advice on how to deal with this kind of failure is given in Figure 6.3.5. Given that shear stresses are calculated based upon the ideal RVSE thickness, characterised by the minimum layers thicknesses (cf. Section 3.4.1), it is proposed to increase the cross section to a 5 layer CLT panel (5x30mm, with alternated orientation). Not only will it decrease the shear stresses (both in-plane and torsional) in the panel, but it will also increase the effective thickness in the vertical direction, from 60 mm to 90 mm: this proposal can therefore potentially solve the tensile failure as well.

With this new cross section, two out of the three failures have been resolved: the design is valid for tension and for torsional shear at the glued interface. However, a slightly high shear stress was still present at the bottom corner ($\tau_v = 4.83 > f_{v,CLT,d} = 4.32$). Since no issue is occurring along the grain, it is unnecessary to increase the thickness of all the layers. With the knowledge gained from Chapter 3, it is possible to increase the ideal thickness in shear by adding an extra 10 mm to the three inner layers. Using this cross section, the complete compliance in strength is fulfilled:

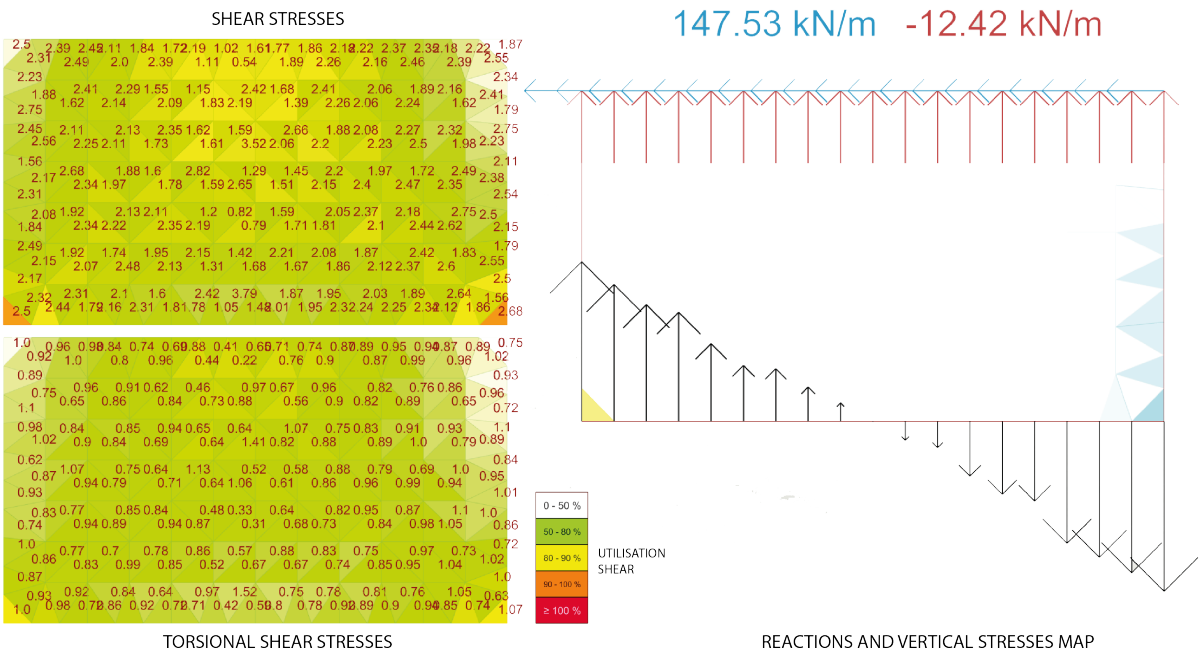

Figure 6.3.7: Reactions, stress maps and values for the final iteration

The shear stress at the bottom corners is still present, but has been decrease from 4.83 to 2.68 MPa. It is also interesting to notice that the wall reactions have evolved as well. With the increase in thickness, the wall also gained in stiffness. Thus, more horizontal loads are directed towards it. The global weight of the structure is also greater. While this increase could have a serious impact on heavy structures such as concrete, the lightness of CLT and its important load bearing capacity counterbalance this issue.

Design of a façade wall with openings

The first wall that has been designed did not feature any openings; the architectural input in this case is limited to increasing the thickness and adjusting the layup of the CLT panel. Nevertheless, the aesthetics of a wall element can have its own impact in some situations. The very first example showed how a different façade design could impact the horizontal stability of a structure; it can also be the case when it comes to strength verification.

For a wall loaded in plane, shear stresses are usually high around openings, as shown in our second example:

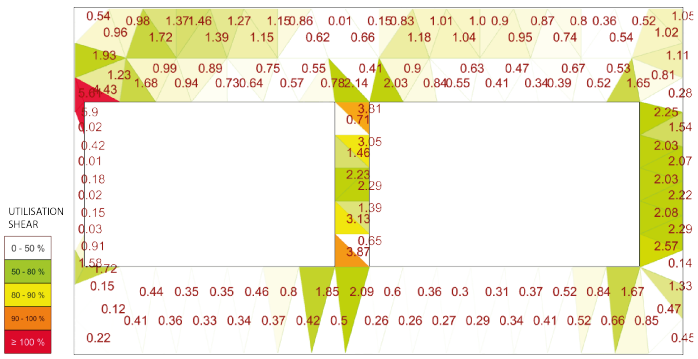


```
SHEAR STRENGTH: NOT SATISFIED
----------------------
Tau v, max = 5.9 MPa (Load Case 2)
fv,d = 4.32 MPa
----------------------
Shear is too high in the wall. To avoid
this:
- Increase the average thickness of
inner layers (both parallel and
crosswise)
- Decrease thickness of cross layers
(not recommended)
- If shear stresses are high around
openings, change opening design, e.g.
avoid narrow wall segments
```

Figure 6.3.8: Shear stress map and values (left) with textual output (right)

At the top left corner, the shear stresses are concentrated and rising up to 5.9 MPa, resulting in a failure. It can also be noted that the wall segment between the two openings are high and close to the actual shear strength (3.87 and 4.32 MPa, respectively). This kind of issue can be, in some situations, solved by a more sensible design which avoids such concentrations, by providing larger wall segments which allow a shear flow in the wall. On this basis, it is proposed to redesign the said wall to give more space around the opening corners:

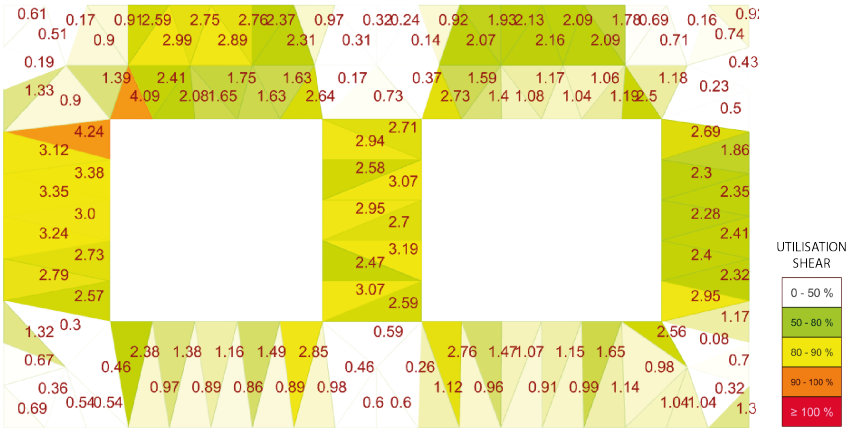

Figure 6.3.9: Shear stress map and values of the corrected design

Around the corner, the shear stress has been reduced to an acceptable value. It must be said that no modification was done regarding the CLT cross-section; only geometrical modifications were tested. In this way, the designer can directly impact the performance of a given wall.

It must be underlined that in this kind of situation, a shear failure is likely to be the issue. Indeed, despite the presence of large openings, the vertical forces flow directly between them, as if the wall was behaving as columns. This obviously adds up to the shear stresses that the wall experiences.

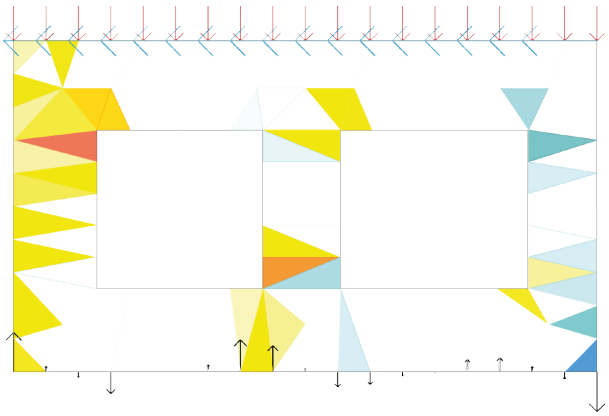

Figure 6.3.10: Vertical stress map (tension / compression), in relative scale

6.3.3 Horizontal elements - Slabs

Finally, it is proposed to move on to the final elements design, i.e. the slabs. Slabs can more or less be designed individually, especially in this framework which does not consider in-plane loads and diaphragm action. Moreover, as explained in Section 5.5, their design is undertaken via a sub-model

component which considers them as spanning in one direction, to counteract the results discrepancies that occur between isotropic and orthotropic modelling.

The slab that is to be designed is therefore assumed pinned along its length, and free at its sides. After the activation of the *Slab Design* component, the floor element can be checked for deflections and strength. In this section, the most critical slab is considered; it has been chosen due to its largest span. On top of the structural loads from the finishes and the structure itself, it is loaded with a variable load of 2.3 kN/m^2, corresponding to a residential occupancy with medium weight moveable partitions; this value varies depending on the load combinations (cf. Framework Manual, Section 6.4). At first, a 3-layer CLT cross section is defined for the slab (3x30mm), yielding the following outputs:

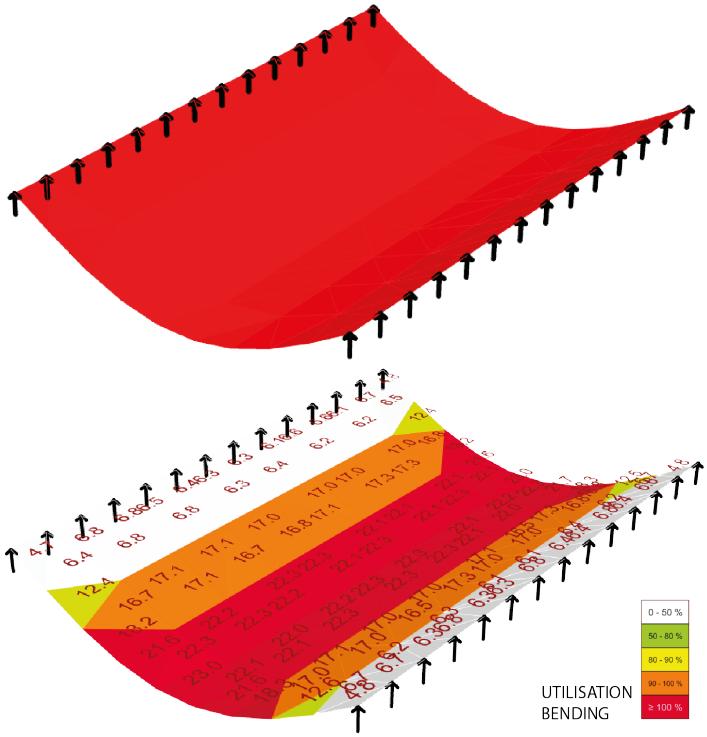


```
DISPLACEMENTS: NOT SATISFIED

w inst = 13.38 mm (Load Case4)
Max. allowed: L / 300 = 20.0 mm
-----------------------------------
w fin = 12.7 mm (Load Case6)
Max. allowed: L / 150 = 40.0 mm
-----------------------------------
w net,fin = 26.08 mm (Load Case4 +6)
Max. allowed: L / 250 = 24.0 mm
-----------------------------------
How to fix this:
- Increase the floor thickness by choosing
another cross section
- Reduce floor span by adding walls (not
recommended)
```

```
BENDING STRENGTH: NOT SATISFIED

Sigma m, max = 23.04 MPa (Load Case 0)
fm,CLT,d =18.19 MPa
----------------------
How to fix this:
- Increase the floor bending stiffness
(KCLT) by choosing another cross section
- Increase the bending strength by
increasing cross section grading from CL24
to CL28
```

Figure 6.3.11: Failure in displacement (top) and bending (bottom) in the considered slab - Stress maps and textual outputs

The wall is failing in bending for the ULS combination with leading imposed load, which usually governs the strength design. Moreover, the SLS characteristic combination yields a too large deflection: the material must be modified. Given the maximum bending stress ($\approx$ 23 MPa), it is unlikely that trading for a CL 28 h grade will give satisfactory results. Moreover, this modification would not impact the bending stiffness of the floor, which does not help with the deflection criteria.

Thus, the only alternative is to increase the bending stiffness of the floor and modify the cross section. Increasing all layers by 10 mm (3x40) is sufficient, in this case, to reduce both bending stresses and deflection to a sufficient level:

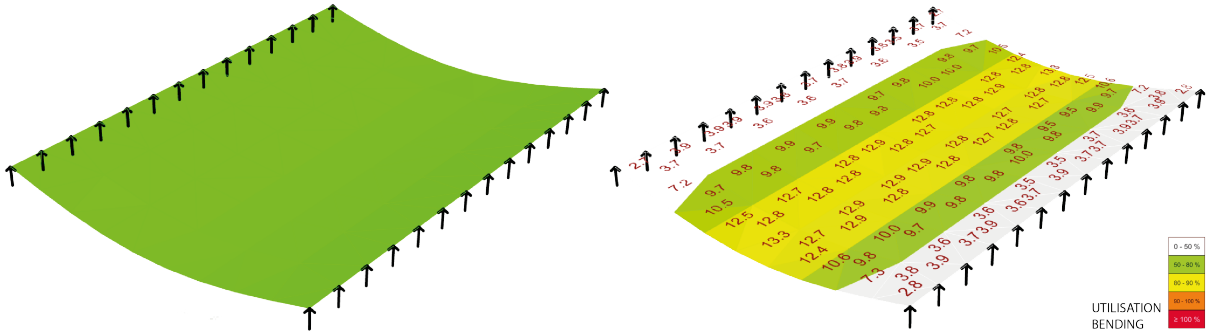


```
DISPLACEMENTS: SATISFIED

w inst = 5.03 mm (Load Case4)
Max. allowed: L / 300 = 20.0 mm
---------------------------------
w fin = 4.93 mm (Load Case6)
Max. allowed: L / 150 = 40.0 mm
---------------------------------
w net,fin = 9.96 mm (Load Case4 +6)
Max. allowed: L / 250 = 24.0 mm
```

```
BENDING STRENGTH: SATISFIED

Sigma m, max = 13.29 MPa (Load Case 0)
fm,CLT,d =17.67 MPa
```

Figure 6.3.12: Validated output after modification of the cross section - Deflection (left) and bending stress map (right)

The results for shear stresses are not displayed here; the floor utilisation in shear is very low compared to the bending behaviour. To provoke a shear failure in the section, the loads were incremented until it failed completely:

```
SHEAR STRENGTH (Second layer from the
midde): NOT SATISFIED

Tau max = 2.59 MPa (Load Case 0)
f_v,d =2.52 MPA
-----------------------------------------
How to fix this:
- Increase the floor bending stiffness
(KCLT) by choosing another cross
section
- Decrease the thickness of parallel
layers (not recommended)
```

```
ROLLING SHEAR STRENGTH (Middle Layer):
NOT SATISFIED

Tau max = 2.59 MPa (Load Case 0)
f_r,d =0.79 MPA
-----------------------------------------
How to fix this:
- Make sure that the chosen layup has a
ratio w / t (board width to thickness
layer) ≥ 4
- Increase the floor bending stiffness
(KCLT) by choosing another cross section
- Decrease the thickness of parallel
layers (not recommended)
```

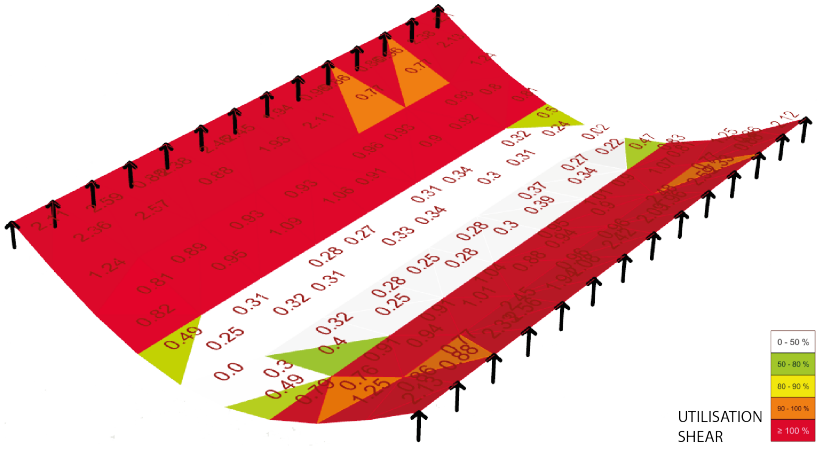

Figure 6.3.13: Failure in shear and rolling shear - Textual output and stress map for the middle layer (rolling shear stresses)

The two outputs give information on the shear and rolling shear stresses in the middle and second to middle layers. This depends on the layup: if the middle layer is crosswise, its rolling shear strength is evaluated, while the second to middle layer is subjected to regular shear stress, and vice versa. In the case shown above, the middle layer is crosswise and therefore subjected to a rolling shear failure. Once again, the solution consists in inflating the bending stiffness of the floor.

Chapter 7

Discussion

The purpose of the work that has been developed during this thesis is to bring the structural design of CLT to the hands of designers, whether they are familiar with this kind of performance assessment or not. Such embedded expertise can be useful only if its framework meets the needs of designers. To evaluate the relevance of the approach, its use has been applied to an existing case study; this allowed for further improvements and evolution. However, it must be noted that feedback from potential users has not been sought yet. The discussion which is the subject of this chapter is based solely on the author's experience.

In his review discussing several model methods and their integration in the early design stages [13], Negendahl compiles a list of criteria from which an evaluation of the approach can be derived. The framework will be intrinsically discussed, and positioned in regard to other methods such as the use of an external structural analysis software (based on the experience with Robot Structural Analysis). Potential improvements of the framework in these fields will be proposed along the way.

The discussion concerns the approach developed within the specific frame of linking a geometry tool with a structural analysis tool in a single environment, and does not deal with the more general comparison of model methods. Furthermore, no consideration is made regarding the inherent ability of the parametric environment to exchange unidirectional information with external BPS tools.

7.1 User experience

7.1.1 User friendliness

Designers tend to favour tools with a user-friendly interface, which are simple to use [13]. The present framework relies on a Visual Programming Interface and is defined by this environment. This implies that the user must be able to grasp the basic principles of such language. This way of using computational algorithms is, in itself, more accessible to non-programmers to the contrary of low-level programming languages like C++. Nevertheless, this nature demands that the users control and handle part of the data manually, by feeding each components with the required inputs. For example, in order to analyse the structural performance of an element, the users must provide the component with the right loads and characteristics of said element. On the other hand, a separate structural analysis software like Robot is able to handle such data seamlessly between the different tasks that it performs.

This framework will therefore be more difficult to grasp in comparison to such software, especially for the first uses since it is necessary to identify the optimised data stream. In order to balance this, a considerable effort has been done to reduce the amount of such manual inputs. They are indeed reduced to global databases containing all the variables for the entirety of the model; those regarding a specific element are retrieved automatically by the components, which means that users simply have to decide which floor or slab they would like to analyse. Moreover, a detailed manual is provided (cf. "Framework Manual", book 2 of the thesis) to guide them through this task.

This setup is inherent to the fact that geometrical data are kept separated from their physical properties and other non-geometrical information, for instance loads. A deeper knowledge in scripting languages, e.g. Python, could greatly improve the framework by reconciling both aspects in a single object.

7.1.2 Knowledge requirement and flexibility

Traditional FEM tools give a great freedom to users to define the structural assumptions of their models, with almost no limitation. The designer is in this case entirely responsible for the results that ensue: this can cause dramatic misjudgements if he/she does not possess a deep understanding of the consequences of a given decision. Typically, this requires a model validation step to make sure that the model indeed reflects realistic situations, and is able to yield correct outputs.

As stated from the very beginning, one objective of the framework is to be accessible for designers or *hybrid practitioners* who do not possess a deep knowledge in structural analysis. To compensate for this potentially missing expertise, the structural assumptions are made on behalf of the designer, as presented in Sections 4.3, 4.5 as well as in the Framework Manual. The same philosophy is applied when it comes to the load application and the calculation of CLT layups in the Excel sheets, where the amount of inputs required from the designers is voluntarily kept to a minimum of trivial data. It must be said that this does not imply, however, that no attention has to be paid to the correctness of the inputs or the assumptions that are made for the model. To help users in this task, the Framework Manual is intended to expose these considerations as exhaustively as possible.

Such guidance and implicit decision making cannot, however, be obtained without sacrificing some flexibility. The actions of the designer in terms of structural considerations are held on a tight rope to ensure the results consistency. Among them is, for example, the fact that connections between elements as well as the base supports are necessarily defined as fixed; such modification is possible in typical FEM tools. In the same fashion as visual programming diminishes the potential of professional developers using low-level languages, this might stray away more experienced users who have the full expertise to make these considerations on their own.

To make the framework attractive to a broader audience, further work is needed to keep this balance while opening up on more flexibility. An example of the direction to follow is showcased in the load applications, in particular for the wind action. By default, users are directed towards a simplified calculation, with three stages of varying wind pressure. As explained in section 4.5 and in the Framework Manual, Section 4.5, wind calculation is more complex than this. An example of a more advanced wind calculation, with a varying pressure storey by storey, is introduced for more experienced professionals. In general, this kind of input part can be easily replaced by more complex considerations, and the Excel framework is simply proposed to provide guidance. The deeper development thus lies in the implementation of this concept, but at a structural modelling level. It is however desirable that such possibility relies on the active participation of the user, and that the default assumptions remain available.

Another aspect of the flexibility is the geometry creation workflow as suggested in the Framework Manual, Section 1. While this can lead to some restrictions if the framework is wished to be applied

on an already established model, which might not share such data structure, it is not considered to be a significant issue. The main requirement lies in the data formatting and structure adopted by the following load application, layup definition and analysis; it is entirely conceivable to create the geometry freely, and then structure it in a similar manner. The proposed approach is however an asset which opens up new perspectives such as automation, which will be discussed later.

7.2 Relevance of the results

7.2.1 Visual feedback and decision support

In a goal to give a better understanding of the results, it is crucial that the framework delivers relevant, communicable visual feedback. This must be even more emphasised when users are not familiar with such results, and might not be able to identify issues within their designs.

The outputs provided by the framework have been presented in Chapter 6. They consist in stress maps and values, as well as textual information to put potential non conformity of the design into the spotlight. Obviously, their exhaustiveness is directly influenced by the nature of CLT structural design, as well as the available data. They can be separated in two main categories: strength and deflections.

Strength outputs, either for walls or floors, are characterised by finite element level outputs. For each finite element (FE) (i.e. face of the generated mesh), the forces it is subjected to are retrieved and processed to calculate the stresses applied in the CLT cross section. This allows the display of stress maps as well as values at the centre of each element. Such visual feedback helps designers to understand the stress repartition in a given object, and to potentially ease these difficulties by carrying out sensible design modifications. Maps are a common output also available in traditional FEM tools. They deliver more information and offer a broader range of effort values; those provided by the framework are however limited by choice and not by unavailability. What the framework seeks to add to this functionality is a less ambiguous representation of the results. In adopting a gradually darker colour, the eye is driven towards more critical regions of the panels, and a FE coloured in red instantly corresponds to a strength failure. The user can (and should) check the textual outputs which inform about the governing stress and the panel resistance. In case of failure, the designer is given advice on how to solve it, either by modifying the CLT panel cross section or its geometry.

Deflection outputs, on the other hand, rely on a global design, and their visual feature is limited to either the confirmation of a satisfactory design (green) or its rejection (red). Once again, textual outputs are available to provide the most critical values and give hints on the decision to take. Such visual outputs are fairly limited and might not provide a broad understanding of the underlying physical phenomenon. They can be, however, completed by the visualisation of the deformation thanks to the Karamba plug-in. This difference with strength outputs is due to the fact that contrarily to stress values, which relates to a surface FE, displacement values concern nodes; visual rendition is therefore more difficult. Moreover, it was preferred to give a straightforward output rather than confuse the user with the display of every single displacement for every single node of the panel / building.

A final type of output, provided only for walls, consists in the support reactions and the global forces acting on the wall. The latter information does not make sense in a structural design perspective, but can be very useful to provide a global understanding of which efforts the element is subjected to. By visually assessing whether a wall is mostly in tension or in compression, as well as the value of the shear force, this feature can help designers grasp how the wall behaves in a broad manner.

It also has its relevance to raise designers' awareness of the global impact of design modifications. For instance, if the user increases the stiffness of a wall by assigning a different CLT cross section, one can immediately notice that the global shear force acting on the wall increases as well, due to the impact on the load distribution.

Obviously, the potential for visual feedback is almost endless, and one could imagine multiple other ways to present such results. However, it is thought that the few examples that have been uncovered offer a good perspective of the framework's capabilities, as well as providing relevant guide to designers through the structural design workflow. The user can therefore make up for potential shortcomings, and hopefully learn the basics of structural analysis and CLT design along the way.

7.2.2 Validity and precision

The approach developed in this thesis does not support yet the definition of orthotropic materials, due to software limitations. Instead, an isotropic modelling of CLT panel has been proposed.

First of all, it is of prime importance to acknowledge than there is no way to approach precisely an orthotropic behaviour with an isotropic material. As shown by the simulations that have been carried out (cf. Chapter 5), the suggested modelling has an influence on the validity of results such as the maximum efforts and displacements in slabs, the load distribution between slabs and walls, as well as the force distribution within wall elements. Regarding slabs, it has been found that depending on the width-to-length ratio, the results given by an isotropic model could be up to 150% below the orthotropic model for shear forces and displacements, and up to 190% for moments. Moreover, it has been seen that orthotropic slabs behave as one-way slabs earlier than their isotropic counterpart, and eventually converge toward a simply supported slab along its length. To compensate for this difference, a sub-model imposing a simply supported slab has been defined, and yields conservative results. Moreover, the contribution from shear to the displacements has been added. In this case, the results that can be obtained from the framework can be considered conservative enough to help the user concluding on a safe design. Secondly, it has been noticed that depending on the ratio of their cross bending stiffness, the load distribution from a slab between 4 walls can be up to 1.45 times higher than in the isotropic model. A correction factor is proposed to be applied to walls defined as "load bearing". Once again, this measure is likely to be conservative. Finally, the force distribution within a wall from vertical and horizontal loads has been evaluated against the ratio of the cross axial stiffness of the orthotropic wall, and the ratio between the orthotropic and isotropic shear stiffness. It has been found that the most influential parameter depends on the ratio between orthotropic and isotropic combined stiffness, and can underestimate the maximum force created by a horizontal load up to 3 times with an isotropic modelling. A function dependent safety factor is introduced to make up for this deficiency.

When assessing such discrepancies, it is difficult to say that the framework gives precise results. At best, it can approximate the values of an orthotropic model and procure conservative values, ensuring a safe design; it cannot however grasp the complexities of the force distribution among orthotropic materials. Moreover, this study has been limited to simple cases and has not been taken to the building scale.

Without further studies to ensure more consistent results, the framework can however find a utilisation to assess the relative performance of several designs, and highlight areas where problems might arise. Moreover, it must be underlined that as soon as orthotropic modelling will be possible within the parametric environment, this research provides all the necessary knowledge for its implementation.

The second observation that will be discussed here concerns the results for the horizontal displacement of the building. First and foremost, the isotropic modelling will also provide underestimated results, for the reason that shear deflections are not included in such calculations in FEM tools. While this is usually not problematic for slender buildings, where bending is governing, the shear stiffness of CLT walls is so low in comparison that this simplification should not be made. This once again could be fixed if orthotropic modelling was made available.

There is however one more issue that needs to be addressed. As explained in Chapter 2, the deformations occurring in the connections have a significant contribution to the displacement. Since in this modelling all the walls are rigidly connected to each other, the final result will not take the relative displacement of walls into account and underestimate the building sway. For instance, in a research led by Xia [47], the displacement of a 40-storey high rise building, featuring CLT shear walls and a concrete core, has been under investigation with the FEM software SAP2000. The process first estimates the displacement of the building under wind loads with rigid connections assumed; it then calculates the necessary connections (brackets) to resist the shear forces on walls, their stiffness, and includes spring elements between walls to represent their actions. It was found that the building displacement was respectively 313mm and 436mm, confirming that connections indeed have a considerable impact.

This can be acceptable in the case of mid-rise timber buildings, as the Puukuokka housing project presented as a case study; at such height, and with a strong structural system such as this one, it is unlikely that horizontal displacements will govern the overall design. This will however gain more and more influence as the height of the building increases, and the wind loading grows stronger; this is an additional reason why the framework is best suited to mid-rise buildings.

If higher structures are to be considered, an approach similar to the one adopted by Xia [47] could be implemented in the future developments of the frameworks. As such, the *Wall Design* component retrieves the base shear force on each individual wall; this value can be used to design the shear connections, which could then be modelled as spring elements. The building design would therefore consist in an iterative process, with the evaluation of a temporary model with rigid connections at first, and the integration of more realistic ones in a second phase.

7.3 Integration in the building design workflow

7.3.1 Support of multiple design iterations

This framework acts as an interface between a geometric model and a structural analysis tool, combining both in a single environment via VPL. Thanks to this specificity, the feedback which is delivered is quasi-instantaneous. Designers can modify their design at will and be informed whether its structural performance has been improved or not. This characteristic has tremendous benefits over the use of an external structural analysis software. First of all, it ensures the consistency, at all time, between the geometric and calculation models; thus reducing the risk of errors. It also suppresses numerous exchanges between software, which will likely occur multiple times during the early design stages. On the other hand, geometry modification is made easier, since the BPS is embedded within a geometric 3D modeller. This criteria has been cited as a favourite among architects, for instance [13].

Such flexibility is not evident with standalone structural analysis software. Complex geometry modelling is less intuitive; this can obviously be improved by using exchange formats such as IFC. Yet, if geometric modification has to be made, users will not only have more difficulties, but also the

changes will not be reflected in the geometric model. This can induce information gaps which can be critical if a solid collaboration framework is not established between model operators.

This framework, and parametric design in general, is therefore considered to be more adapted to the support of multiple design iterations, especially in the early design stages.

7.3.2 Framework scalability

The scalability represents the ability of the approach to adapt to different design stages, and accommodate an increasing quantity of information as the design evolves [13]. The framework, as developed to this day, is mostly oriented towards the early design stages. It is a simplified tool which does grab the essence of a design, and produces a representation of its structural system. However, this is also the case with typical calculation models due to BPSs' limited ability to handle complex geometry. Moreover, such simplification can yield satisfactory results while reducing the calculation time; simplification might therefore not be an issue.

Nonetheless, in order to enhance the use of such approach in later stages, one suggestion could be to offer the possibility to model the connections between the different structural elements. In this way, the behaviour of the building would be more precise as more structural details are available.

7.4 Further studies

Obviously, the framework as introduced in this report does not have the ambition to be a finished product. A considerable amount of improvements, additions and general validity must be investigated for the framework to operate at its full potential. Some of them are suggested above, and further studies can emerge from them.

7.4.1 Improvements to the framework - designers feedback

One aspect that has not been considered yet is whether the proposed methodology indeed meets the needs of the target users, i.e. designers. The discussion developed above is based on the author's experience and might not reflect what the actual users are looking for. To enhance this aspect, it can be beneficial to seek designers' feedback regarding this methodology to approach the design of CLT. Such study can bring improvements in areas such as user experience, better integration within the designers' practices, as well as directed visual feedback and decision help that give more relevant answers to the users interrogations.

This could include the trial of the framework on a panel of designers, but is also an invitation to a wide collaboration in the early design phases.

7.4.2 Improvements of the results

As explained above, the framework as such is not in a position to deliver sufficiently accurate results, and can at best provide designers with overestimated results.

This is due to the fact that so far, the modelling of orthotropic results is not available in the Grasshopper environment: this would be the most correct way to reflect a realistic behaviour of CLT buildings. In the meantime, it can be interesting to further explore whether a finer approach of equivalent isotropic modelling is viable. This could include the discrepancy in behaviour of walls with openings, as well as a more global characterisation at the building scale.

Another point that challenges the validity of the results is that the connections between CLT elements are not modelled. This underestimates the calculated horizontal deflection of the building. To correct this result, a way to integrate such parameters in the calculation must be investigated, which respects the philosophy of the framework and its integration in the early design phases.

7.4.3 A step towards automation

The framework opens up new possibilities towards automation in designing CLT buildings and creating geometry. Automation can provide designers with a support in multi-criteria decision making and sensitivity analysis, among others [13]. In a goal to provide enhanced design support, a final suggestion for further studies is to develop this aspect of the parametric framework.

As such, some of the components of this framework define an embryo of shape grammar, which establish rules between geometrical elements [13]. For instance, disabling the "Keep Shape" option (cf. Framework Manual, Section 2.2), the geometry of the wall is constrained within the boundaries of the *Frame*. Such rules impose limits on the possible geometrical spectrum, which can be understood by multi-criteria optimisation algorithms.

A further evolution of this shape grammar could result in evaluations such as: what is the most optimised layout for stabilising elements, to provide an acceptable horizontal deflection while minimising the amount of walls?

The answer to this question, in the context of massive timber construction, could open up to hybrid structures where some of the CLT walls are replaced by a Glulam frame structure, i.e. beams and columns. This would further decrease the material consumption, and help the design of more sustainable structures.

Chapter 8

Conclusion

Massive timber structures incarnate a significant progress towards more sustainable buildings that will shape our future. Among them, this work has been focusing on the particular case of Cross Laminated Timber. CLT makes up for strong, large scale structural elements which, thanks to their high dimensional stability and light weight, represent a high value alternative to mineral construction materials.

Gathering knowledge about the behaviour and structural design of this relatively new material, derived from the research undertaken by TU Graz, served as the foundation to a framework aiming at bridging architectural and structural design of Cross Laminated Timber.

The framework develops an approach to the design of CLT panels inspired by current prefabrication and modular systems, combining geometric and calculation models by mean of a visual programming interface, within an integrated dynamic model. Oriented towards the early design stages, this allows to perform structural tasks in an environment that increasingly more designers are familiar with, which has been devised to be as flexible and user-friendly as possible. It furthermore provides support for the multiple iterations that the design goes through at the very beginning of a project.

With the results that are currently available, users can assess the horizontal stability of the building, as well as design CLT panels used as walls and floors. The structural evaluation of the design is performed under the assumption of an isotropic behaviour of CLT panels, which limits the validity of the results that ensue. Indeed, a more correct modelling of such material is inherently orthotropic. In particular, the vertical load distribution from slabs to walls is likely to cause significant discrepancies, as well as the horizontal load distribution from, for instance, wind loading. In compensation, this influence has been evaluated by comparative simulations between isotropic and orthotropic models, in an attempt to propose correction factors. While not reflecting with precision the behaviour of CLT buildings, the application of such factors can lead to a safe, though not optimised, structural verification. Furthermore, the influence of connections on the horizontal displacements are not taken into account, which results in underestimations.

Ultimately, the framework supports the ambition of raising more awareness about CLT materials and encourage designers to choose such structural system over more familiar ones. All along the implementation of the framework, the user is guided through the characteristics of CLT products and their structural design. The acquired knowledge, combined to the flexibility of the framework, puts the user in an active position to customise its own CLT products, and to free him/herself from manufacturer specifications. A wide range of visual feedback, along with advice on the modifications that can be considered to solve potential structural issues, further aims at strengthening this approach.

Whether such tool can actually encourage and promote CLT structures among designers is debatable, and is obviously not sufficient in itself to accomplish this task. Nevertheless, it represents a step towards making CLT structural design accessible to a broader audience.

Bibliography

[1] Sven Thelandersson, Erik Aasheim, and Alpo Ranta-Maunus. *New timber construction in Nordic countries. Keynote presentation.* eng. 2004.

[2] Timber Design & Technology. *Treet: the tallest timber-framed building in the world*. [Online; accessed 18-June-2017]. 2015. URL: http://www.timberdesignandtechnology.com/treet-the-tallest-timber-framed-building-in-the-world/.

[3] Catherine Rowell. *Europe's largest cross laminated timber structure built in Norway*. [Online; accessed 18-June-2017]. 2016. URL: http://www.constructionglobal.com/major-projects/europes-largest-cross-laminated-timber-structure-built-norway.

[4] Eleanor Gibson. *White Arkitekter selected to build timber-framed high-rise in Sweden*. [Online; accessed 18-June-2017]. June 2016. URL: https://www.dezeen.com/2016/06/07/kulturhus-i-skelleftea-white-arkitekter-cultural-centre-hotel-sweden-wooden-timber-frame/.

[5] MDH. *Moholt Student Village Masterplan*. [Online; accessed 18-June-2017]. 2017. URL: https://mdh.no/project/moholt-student-village/.

[6] D. Horswill and T. Nielsen. "Can CLT construction help Copenhagen become world's first carbon neutral city?" In: *Structures and Architecture: Beyond their Limits*. Third international conference on structures and architecture. (Guimaraes, Portugal,). Ed. by Paolo J.S. Cruz. CRC Press, 2016. ISBN: 9781317549956.

[7] Annie Gosselin et al. "Main motivations and barriers for using wood as a structural building material–a case study". In: *11e Congrès International de Génie Industriel–CIGI2015*. (Québec, Canada). 2015.

[8] Katarina Brandt. "CLT – the future has historic roots". In: *Wood Magazine, Issue 4*. 2015. URL: http://www.swedishwood.com/wood-magazine/2015-4/clt_the_future_has_historic_roots/.

[9] Tobias Schauerte. "Wooden house construction in Scandinavia-a model for Europe". In: *Internationales Holzbau-Forum (IHF 2010); International Wood Construction Conference (IHF 2010)*. Eberl Print GmbH. 2010, pp. 1–10.

[10] Omar Espinoza et al. "Cross-laminated timber: status and research needs in Europe". In: *BioResources* 11.1 (2015), pp. 281–295.

[11] *Timber structures – Cross laminated timber – Requirements*. Standard. European Commitee for Standardization, 2015.

[12] *Eurocode 5: Design of timber structures — Part 1-1: General — Common rules and rules for buildings*. Standard. European Commitee for Standardization, 2008.

[13] Kristoffer Negendahl. "Building performance simulation in the early design stage: An introduction to integrated dynamic models". In: *Automation in Construction* 54 (2015), pp. 39–53.

[14] STED Network. *Home*. [Online; accessed 21-June-2017]. 2017. URL: http://stednetwork.org.

[15] Reinhard Brandner et al. "Production and Technology of Cross Laminated Timber (CLT): A state-of-the-art Report". In: *Focus Solid Timber Solution - European Conference on Cross Laminated Timber (CLT)*. Graz University of Technology, Austria. 2013, pp. 3–36.

[16] Stora Enso. *CLT - Cross Laminated Timber*. [Online; accessed 18-June-2017]. 2013. URL: http://www.clt.info/en/product/.

[17] Sylvain Gagnon and Ciprian Pirvu. *CLT Handbook-Canadian Edition*. 2011. ISBN: 978-0-86488-547-0.

[18] R Brandner et al. "Cross laminated timber (CLT): overview and development". In: *European Journal of Wood and Wood Products* 74.3 (2016), pp. 331–351.

[19] Stora Enso. *Building systems by Stora Enso - 3-8 Storey modular element buildings*. 2016.

[20] Stora Enso. *Stora Enso CLT - Wood: the world's oldest and yet most modern building material*. 2016.

[21] Anne Kirkegaard Bejder. "Aesthetic qualities of cross laminated timber". PhD thesis. Aalborg University: Department of Civil Engineering, 2012.

[22] R. Harris. "8 - Cross laminated timber". In: *Wood Composites*. Ed. by Martin P. Ansell. Woodhead Publishing, 2015, pp. 141–167. ISBN: 978-1-78242-454-3. DOI: https://doi.org/10.1016/B978-1-78242-454-3.00008-1. URL: http://www.sciencedirect.com/science/article/pii/B9781782424543000081.

[23] Rothoblaas. *Wood connectors and timber plates*. 2015.

[24] Massimo Fragiacomo. "Seismic behaviour of cross-laminated timber buildings: numerical modelling and design provisions." In: *Focus Solid Timber Solution - European Conference on Cross Laminated Timber (CLT)*. The University of Bath. 2013, pp. 166–182.

[25] Helene Unterwieser and Gerhard Schickhofer. "Characteristic values and test configurations of CLT with focus on selected properties". In: *Focus Solid Timber Solution - European Conference on Cross Laminated Timber (CLT)*. Graz University of Technology, Austria. 2013, pp. 53–73.

[26] *Timber structures – Glued laminated timber and glued solid timber – Requirements*. Standard. European Commitee for Standardization, 2013.

[27] Reinhard Brandner et al. "Shear properties of Cross Laminated Timber (CLT) under in-plane load: test configuration and experimental study". In: *Proceedings of the 2nd International Network on Timber Engineering Research meeting*. 2015.

[28] Thomas Ehrhart et al. "Rolling shear properties of some European timber species with focus on cross laminated timber (CLT): test configuration and parameter study". In: *Proceedings of the 2nd International Network on Timber Engineering Research meeting*. 2015.

[29] Reinhardt Brandner and Gerhard Schickhofer. "Properties of cross laminated timber (CLT) in compression perpendicular to grain". In: *1st INTER-Meeting, Bath*. 2014.

[30] Thomas Bogensperger, Thomas Moosbrugger, and Gregor Silly. "Verification of CLT-plates under loads in plane". In: *11th World Conference on Timber Engineering (WCTE2010), Riva del Garda*. 2010.

[31] *Eurocode - Basis of Structural Design*. Standard. European Commitee for Standardization, 2010.

[32] Hans Joachim Blass and Peter Fellmoser. "Design of solid wood panels with cross layers". In: *8th world conference on timber engineering*. Vol. 14. 17.6. 2004.

[33] Alexandra Thiel. "ULS and SLS design of CLT and its implementation in the CLTdesigner". In: *Focus Solid Timber Solution - European Conference on Cross Laminated Timber (CLT)*. Graz University of Technology, Austria. 2013, pp. 77–102.

[34] Thomas Moosbrugger, Werner Guggenberger, and Thomas Bogensperger. "Cross-Laminated Timber Wall Segments under homogeneous Shear with and without Openings". In: *Proceedings of the 9th World Conference on Timber Engineering*. 2006.

[35] Stora Enso. *Stiffness matrix for Stora Enso CLT*. 2015.

[36] Kristoffer Negendahl, Toke Rammer Nielsen, and Ole Schrøder. "Consequence Based Design. An approach for integrating computational collaborative models (Integrated Dynamic Models) in the building design phase". PhD thesis. Technical University of Denmark, Department of Civil Engineering, 2016.

[37] Milena Stavric, Predrag Sidanin, and Bojan Tepavcevic. *Architectural scale models in the digital age - design, representation and manufacturing*. Springer, 2013. ISBN: 978-3-7091-1447-6.

[38] Clemens Preisinger. "Linking Structure and Parametric Geometry". In: *Archit Design*. Vol. 83. 2013, pp. 110–113. DOI: 10.1002/ad.1564.

[39] Tood R. Beyreuther. "Next generatio CLT: Mass-customization of hybrid composite panels". In: *GLOBALIZING ARCHITECTURE / Flows and Disruptions*. Ed. by John Stuart and Mabel Wilson. Association of Collegiate Schools of Architecture. 2014, pp. 866–872.

[40] Clemens Preisinger. *Karamba - User manual for version 1.2.2*. 2016.

[41] *Eurocode 1: Actions on structures — Part 1-4: General actions — Wind actions*. Standard. European Commitee for Standardization, 2009.

[42] *Eurocode 1 — Actions on structures — Part 1-3: General actions — Snow loads*. Standard. European Commitee for Standardization, 2009.

[43] Md Shahnewaz et al. "In-plane stiffness of CLT panels with and without openings". In: *Proceedings of the World Conference on Timber Engineering 2016*. (Vienna, Austria,). 2016.

[44] Vahid Mahdavifar, Andre R Barbosa, and Arijit Sinha. "Nonlinear layered modelling approach for cross laminated timber panels subjected to out-of-plane loading". In: 41st IAHS WORLD CONGRESS - Sustainability and Innovation for the Future. (Albufeira, Algarve, Portugal). 2016.

[45] Zoé Tolszczuk-Leclerc et al. "Design process of a free-form structure using CLT panels - Analysis of an architectural large scale structure". In: *Proceedings of the World Conference on Timber Engineering 2016*. (Vienna, Austria,). 2016.

[46] Office for Peripheral Architecture OOPEAA. *Puukuokka Housing Block*.

[47] Zhouyan Xia. "Numerical Analysis of Wood-Concrete Skyscraper by Using Spring Elements to Simulate Mechanical Connections". In: ().

Modular Timber Structures with Parametric Design Frameworks

BOOK 2 - Framework Manual

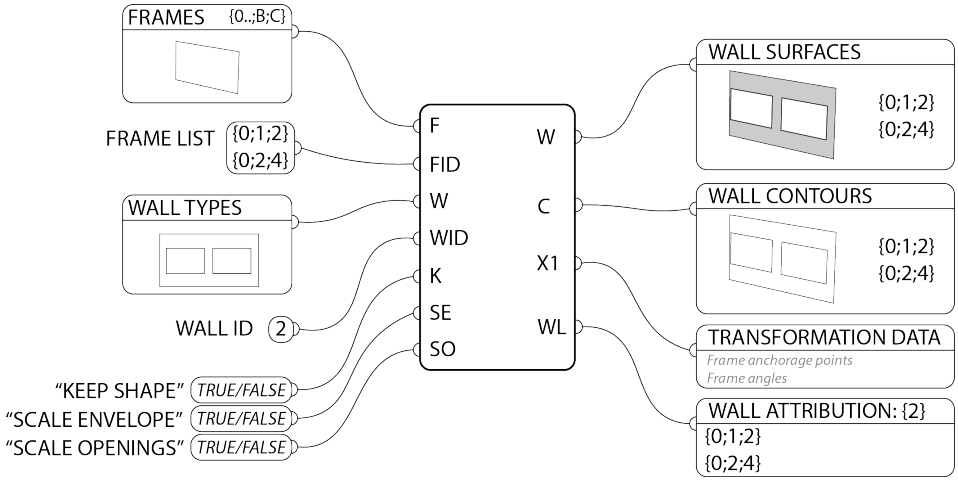

Master Thesis Project

Simon Clavelin

June 2017

Technical University of Denmark
Department of Civil Engineering
Brovej, Building 118
2800 Kgs. Lyngby
Denmark

Author:

Simon Clavelin
s151369

Supervision:

Kristoffer Negendahl
Department of Civil Engineering

Preface

This book forms the second part of the Master Thesis entitled "Modular Timber Structures with Parametric Design Frameworks", submitted as partial fulfilment of the requirements to the obtention of the degree of Master of Science in Architectural Engineering, from the Technical University of Denmark.

It exposes the framework methodology and details the Grasshopper components that have been developed within the parametric environment.

Kongens Lyngby, June 23rd, 2017

Simon Clavelin

Contents

List of Figures

List of Tables